In Vivo Mercury (De)Methylation Metabolism in Cephalopods under Different p CO 2 Scenarios

Sophie Gentès, Antoine Minet, Christelle Lopes, Emmanuel Tessier, Claire Gassie, Remy Guyoneaud, Peter Swarzenski, Paco Bustamante, Marc Metian, David Amouroux, et al.

In vivo mercury (de)methylation metabolism in cephalopods under different pCO_2 scenarios

Sophie Gentès *[a,c], Antoine Minet [a], Christelle Lopes [b], Emmanuel Tessier [c], Claire Gassie [c], Rémy Guyoneaud [c], Peter W. Swarzenski [d], Paco Bustamante [ae], Marc Metian [d], David Amouroux [c], Thomas Lacoue Labarthe [a].

[a] LIENSs, UMR 7266 CNRS-La Rochelle Université, 2 rue Olympe de Gouges, 17000 La Rochelle, France.

[b] Univ Lyon, Université Lyon 1, CNRS, Laboratoire de Biométrie et Biologie Evolutive UMR 5558, 69622 Villeurbanne, France

[c] Université de Pau et des Pays de l'Adour, E2S UPPA, CNRS, IPREM UMR 5254, Pau, France

[d] Radioecology Laboratory, International Atomic Energy Agency, Marine Environment Laboratories, Monaco 98000.

[e] Institut Universitaire de France (IUF), 1 rue Descartes 75005 Paris, France

Author for correspondence, e-mail: so.gentes@gmail.com

Declarations of interest: none

Synopsis: Experimental *in vivo* mercury metabolism was studied in a model cephalopod under low pH conditions (i.e., effects of ocean acidification).

Abstract: This work quantified the accumulation efficiencies of Hg in cuttlefish, depending on both organic (MeHg) and inorganic (Hg(II)) forms, under increased pCO_2 (1600 µatm). Cuttlefish were fed with live shrimp injected with two Hg stable isotopic tracers ($Me^{202}Hg$ and $^{199}Hg(II)$), which allowed for the simultaneous quantification of internal Hg accumulation, Hg(II) methylation and MeHg demethylation rates in different organs. Results showed that pCO_2 had no impact on Hg bioaccumulation and organotropism, and both Hg and pCO_2 did not influence the microbiota diversity of gut and digestive gland. However, the results also demonstrated that the digestive gland is a key organ for *in vivo* MeHg demethylation. Consequently, cuttlefish exposed to environmental levels of MeHg could exhibit *in vivo* MeHg demethylation. We hypothesize that *in vivo* MeHg demethylation could be due to biologically induced reactions or to abiotic reactions. This has important implications as to how some marine organisms may respond to future ocean change and global mercury contamination.

Keywords: enriched isotopes, microbiota, cuttlefish, acidification, methylmercury, inorganic mercury.

1. Introduction

Mercury (Hg) in the ocean has tripled since the pre-industrial era [1], through river discharges, atmospheric deposition, and the uptake of inorganic Hg (Hg(II); [2]. A fraction of this Hg(II) can be converted to methylmercury (MeHg) mainly by anaerobic bacteria, a form that is well known to efficiently bioaccumulate and biomagnify in some biota [3,4] and can be highly toxic, especially to the nervous system [5,6]. Mechanisms of Hg toxicity are difficult to fully understand as pathways and reactions can be unique at the species level, the chemical form of Hg, as well as environmental conditions [7-9], such as the ocean acidification. Due to the anthropic growing release of carbon dioxide (CO_2) in the atmosphere, surface ocean partial pressure of carbon dioxide (pCO_2) is increasing, causing a projected reduction of seawater pH by 0.2–0.4 units over this century [10]. A growing body of works focused on the effect of ocean acidification on the bioaccumulation and toxicity of metal contaminants (e.g. [11,12]. Thus, seawater hypercapnia led to disturbances of the ionic and acid-base balances, the energy metabolism, feeding and digestive physiology [13-15] and thus could affect organism's ability to deal with pollutants.

Among marine organisms, cephalopods, including cuttlefish, are inexorably exposed to coastal chemical contamination and to the elevated pCO_2 currently recorded in these coastal waters [16] during key stages of its life cycle (e.g. embryonic and juvenile life). Their abilities to upregulate the acid-base balance under hypercapnia conditions are expected to affect the metal bioaccumulation efficiencies in juveniles (e.g. [17,18]). In addition, cephalopods have a central position in coastal food webs as both predator and prey for numerous species of fish of interest (e.g. sea bass, meagre fish, etc...), birds and marine mammals (e.g. pilot whales), making them an efficient integrator and vector of contaminants in the biota.

Regarding Hg, these animals demonstrate efficient bioaccumulation of Hg despite their relatively short life span, which limits Hg levels in their tissues. Overall, benthic cephalopod

species displayed higher Hg concentrations than pelagic species (i.e., Sepiidae and Octopodidae, 480 and 380 ng g^{-1} dw respectively vs Ommastrephidae and Loliginidae, 360 and 260 ng g^{-1} dw respectively) [19], possibly due to their proximity to seabed sediment where Hg can be methylated [20,21]. In most cephalopod species, Hg concentrations are positively correlated with age and size (e.g. [22]) and often associated with increasing trophic position [23-25]. These observations are consistent with the fact that food is the main Hg bioaccumulation pathway in these species [19,26]. The Hg tissue distribution in cephalopods indicates that the highest concentrations of total Hg (MeHg + Hg(II)) were usually found in the muscle mantle (more than 70% of the total Hg measured in the whole body), followed by the digestive gland [27-30]. Most of the Hg found in the digestive gland is Hg(II), in contrast to the large proportion of organic mercury (MeHg) found in muscle tissues (e.g. [27,31]). This organotropism suggests that dietary MeHg is translocated from the digestive gland to the muscles due to the high affinity for the sulfhydryl groups present in muscular proteins but also that an *in vivo* demethylation of organic Hg could occur in the digestive gland [32]. Known to arise in the liver of mammals and birds, very few studies investigated demethylation and its reverse process in digestive organs (digestive gland/liver, gut) of aquatic organisms (e.g. [33,34]). In the black seabream, *Acanthopagrus schlegeli*, demethylation was efficient in both the gut and liver, but was 600-fold higher in the former [35], suggesting a key role for microbiota in this Hg transformation. In turn, *hgc* genes encoded for enzymatic systems involved in methylation process have been identified in the gut microbiota of both vertebrates and invertebrates [36]. Methylation has been demonstrated in isolated intestines of freshwater fish [33] and in living tilapia, although negligeable relative to the ingested Hg concentration [34]. All these cues defined the involvement of microbiota in Hg transformations as a research priority [37] as it could modify Hg internal toxicity for organisms

In the future ocean, increased seawater pCO_2 could impact both Hg dynamic and microbiota activity. Indeed, the trophic Hg bioaccumulation tends to be hampered with hypercapnia in both meagre and sole [38,39]. In addition, elevated pCO_2 leads to intestinal dysbiosis in the seabream affecting the microbiome diversity [40] and thus, the *in vivo* Hg transformations.

This study broadly investigates the microbially mediated *in vivo* (de)methylation transformation reactions of ingested Hg(II) and MeHg in cephalopods, under elevated pCO_2. Specifically, this work traces Hg(II) and MeHg trophic pathway within the common cuttlefish *Sepia officinalis* as a model, using a double tracer approach based on i) stable isotopic tracers ($Me^{202}Hg$ and $^{199}Hg(II)$) that permits concurrent quantification of MeHg and Hg(II) organotropism as well as internal (de)methylation processes, and ii) microbiota analyses via the 16S rRNA gene to assess possible *in vivo* bacterial transformations of Hg in digestive organs. Analyses were performed at different kinetic points (0,10, 20 and 30 days) on several tissues but take into account the whole organism in order to obtain a Hg mass budget. The exposure parameters are based on environmentally realistic values: isotopic tracers allow to contaminate food (live shrimps) in the $ng.g^{-1}$ range and pCO_2 value is defined on the most pessimistic scenario of anthropogenic CO_2 emissions [41-43] resulting to more than a doubling in ocean acidity (1600 µatm). A multi-compartments toxico-kinetic (TK) model was developed and fitted to all organ concentrations simultaneously to describe the organotropism and fate of MeHg and Hg(II) in cuttlefish over time.

2. Materials and Methods

2.1 Sampling of the cuttlefish

Roughly 1 month old juvenile common cuttlefish (*Sepia officinalis)* were caught by dipnet in Arcachon Bay (Atlantic coast of south-western France; 44° 41'14.0" N; 1° 14'00.6" W) in June 2019 and were transported in an aerated tanks to the IAEA marine laboratories in Monaco. From their capture until the end of the experiment, cuttlefish were exclusively fed with wild, live shrimp (*Palaemon varians)* caught from a single fishing site on the French Atlantic coast (46° 12'18.0" N; 1° 11'42.0" W). Shrimp were fed with commercial shrimp food prepared from bycatch marine products (® Ocean Nutrition Formula One).

2.2 Experimental design

All procedures were approved by the French national ethic committee (approval number APAFIS # 20520-2019050614554709). Upon arrival, cuttlefish with similar size (mantle length: 2.66 ± 0.03 cm at initial time; n = 72) were transferred into eight 20 L black plastic tanks (n = 9 per tanks). They were maintained in open circuit (flux: 20 L h^{-1}; salinity: 38; temperature: 19 ± 0.2°C; pH: 8.0 ± 0.1; 12h light:12h dark cycle) and the pH of four tanks were progressively lowered by bubbling CO_2 on a 2.5 days period until reaching a pH of ~7.6 (i.e., acidified condition: pH = 7.54 equivalent to 1600 µatm), consistently with modelled scenarios of ocean pH at the end of the century (i.e., SSP5-8.5, [44]). The other four tanks were maintained at ambient pH all along the experiment. Details about pCO_2 regulation and monitoring are explained in [26] Minet et al. (2022).

After one week of acclimatization, the experiment started for a period of 30 days during which cuttlefish were fed with 1) live shrimp at ambient pH (pH 8.1; equivalent to 400 µatm) (control condition), 2) $Me^{202}Hg$ and $^{199}Hg(II)$ injected-live shrimp at pH 8.1 (Hg condition), 3) live shrimp at acidified pH 7.54 (equivalent to 1600 µatm) (pH condition), 4) $Me^{202}Hg$ and $^{199}Hg(II)$ injected- live shrimp at pH 7.54 (Hg+pH condition).

Each cuttlefish was daily fed 3 shrimps that corresponded to 5% of the cuttlefish wet weight (shrimps average weight: 0.146 ± 0.034 g dw; natural Hg concentrations: 8 ± 1 ng $Me^{200}Hg.g^{-1}$ and 38 ± 4 ng $^{200}Hg(II).g^{-1}$ dw, 15 ± 3% MeHg, n=27). For cuttlefish of the Hg and Hg+pH conditions, the first shrimp of the day was $Me^{202}Hg$ and $^{199}Hg(II)$-contaminated (named Hg-contaminated shrimp below) and the others two served as a food supplement to fulfill nutritional requirements (food given in two parts). The Hg contaminated shrimp were intramuscularly injected with 5 µl of the Hg solution containing 8.7 ng $^{199}Hg(II)$ (solution: 1731 ng $^{199}Hg(II).g^{-1}$) and 7.4 ng $Me^{202}Hg$ (solution: 1475 ng $Me^{202}Hg.g^{-1}$). Shrimp injection procedures and details on the experimental design are described in the Supplementary Information in section 1.1 and 1.2. The injection of Hg allowed at keeping as constant as possible the contamination pressure for each cuttlefish, avoiding the elimination and potential internal biotransformation of Hg by shrimp, in particular Hg demethylation. In turn, Hg was expected to be more metabolically available, being not strongly bound to proteins or cell components involved in the Hg metabolism. However, we hypothesized that, although being more labile, Hg metabolism (transport, transformation, binding) would be close to this naturally contained in the shrimp tissues. The theoretical quantity of Hg absorbed per cuttlefish throughout the experiment was reported in Table S1. The loss and possible transformations of Hg stable isotopes in shrimp was assessed immediately, 10 min, 3h and 5h after injection (Table S2). To maximize and maintain a healthy water quality and to minimize potential contamination from recycling of Hg, tank bottoms were cleaned every day by eliminating cuttlefish feces and food remains. Cuttlefish were sampled after 10, 20 and 30 days for control and Hg conditions, and for 10 and 30 days for pH and Hg+pH conditions. Mantle muscle (without skin), gut, digestive gland, gills, brain (optic lobes) and the remaining tissues (but the cuttlebone) of collected individual were independently harvested in their entirety. The gut and digestive gland of cuttlefish were collected in sterile cryotubes and stored at −80 °C: one part being used to study the microbial

diversity by MISEQ analysis; a second part was stored until Hg speciation analysis. The rest of samples was stored at −80 °C until Hg speciation analysis.

2.3 Hg speciation analysis

The different tissues of cuttlefish and whole shrimp were digested with 6N HNO_3 using microwave digestion, as previously described [45]. Hg species were determined by GC-ICP-MS (gas chromatography-inductively coupled plasma-mass spectrometry; Trace GC and ICPMS X2 series, Thermo Fisher) as detailed elsewhere [45,46]. Each assay was analyzed in triplicate, with the analytical uncertainty error for MeHg and Hg(II) being <22%. Data quality was checked by blanks. The limits of quantification were 1.5 $ng.g^{-1}$ for Hg(II) and 1.3 $ng.g^{-1}$ for MeHg. The method used to calculate Hg species concentrations, (de)methylation yields has been described previously by [47]. Briefly, the amounts of Hg species deriving from the enriched isotopes 199 and 202 ($Me^{199}Hg$, $Me^{202}Hg$, $^{199}Hg(II)$, $^{202}Hg(II)$) were determined by species specific isotopic dilution using isotopic pattern deconvolution methodology [47]. The methylation potential was calculated by dividing the amount of newly formed $Me^{199}Hg$ by the sum of the amount of remaining spiked $^{199}Hg(II)$ and newly formed $Me^{199}Hg$. The demethylation potential was calculated by dividing the amount of newly formed $^{202}Hg(II)$ by the sum of the amount of remaining spikled $Me^{202}Hg$ and newly formed $^{202}Hg(II)$. As tissues and organs were harvested in their entirety and weighed, results could be expressed in quantity of Hg (ng) per organ (on a dry weight basis), in addition to being expressed in concentrations ($ng.g^{-1}$ dw).

2.4 MiSEQ Analysis

DNA extractions were performed according to the Dneasy PowerSoil Kit (QIAGEN, France) following the manufacturer instructions from 60 to 190 mg of gut and 120 to 440 mg of digestive gland. PCR amplifications were performed with the universal eubacterial 16S rRNA gene primers 8F, 5′- AGAGTTTGATCCTGGCTCAG-3′ and 1492R, 5′-GGTTACCTTGTTACGACTT -3′. Then nested PCR amplifications was needed and were performed on the first PCR products. The V4–V5 hypervariable region of the 16S rRNA gene targeting bacteria and archaea was amplified using the primers 515F, 5′-GTGYCAGCMGCCGCGGTA-3′ and 928R, 5′-CCCCGYCAATTCMTTTRAGT-3′. The reaction mixture and the cycle conditions are detailed in sup data. Illumina MiSeq 250 bp paired-end sequencing was performed by the Get-PlaGe sequencing service (INRA, Toulouse, France). MiSEQ sequences obtained were deposited in the GenBank DNA database of the National Center for Biotechnology Information (http://www.ncbi.nlm.nih.gov) under accession numbers SUB12268361 (BioProject PRJNA900433). Sequence analysis was done with the pipeline FROGS from the Galaxy portal of the Toulouse Midi-Pyrenees bioinformatics platform [48,49] (details in sup data, section 1.3).

2.5 Data analyses

2.5.1. Mercury toxico-kinetic model

A multi-compartments toxico-kinetic model was developed, considering that (i) uptake occurs only from intestines; (ii) intestines and gills can eliminate Hg; (iii) all tissues are connected to each other and thus MeHg and Hg(II) can transfer from one to another; (iv) methylation and demethylation can occur in all tissues; and (v) dilution by growth occurs in all organs according to their respective growth rate. The global scheme is represented in Figure 1 and the corresponding ordinary differential equations are detailed in Supporting Information in section 1.5. Bayesian inference was used to fit the model to all data simultaneously (MeHg and Hg(II)

concentrations in all tissues and weight of them during time), according to the method detailed in [50].

2.5.2. Statistical analyses

Factorial ANOVAs were used to compare biotic and abiotic factors (e.g., weight, size, Hg concentrations, etc…) between experimental conditions or organs, after checking the assumptions of normality and homoscedasticity of the error term. If the assumptions were not satisfied, the non-parametric Mann-Whitney test was used. If the factorial ANOVAs were significant, the parametric post hoc LSD Fisher test was applied. Comparisons of means for two different conditions (e.g. quantity of MeHg in gut and in digestive gland after 30 days of exposure) were performed using Student's t-test when the assumptions were met or the non-parametric Wilcoxon test when they were not. In each test, $p < 0.05$ was considered significant. All statistical investigations were performed using STATISCA version 6.1 software.

3 Results

3.1 Effects of seawater acidification on Hg metabolism

Bioaccumulation and transformation of isotopically enriched Hg compounds (Hg(II), MeHg) were measured in gut, brain, mantle, digestive gland and the remaining tissues of cuttlefish under two pH conditions (8.1 and 7.54) after 10 and 30 days of exposure. The results of the statistical tests comparing the different variables at both pH values are summarized in Table S3 for the 10-day exposure and in Table S4 for the 30-day exposure. No significant differences were observed between both pH conditions except a higher concentration of $Me^{202}Hg$ associated with the lowered pH: 1) in brain at 10 days (53.2 ± 15.8 and 30.1±10.8 $ng.g^{-1}$ at pH 7.54 and 8.1, respectively), 2) in mantle at 10 days (34.4 ± 5.1 and 19.2 ± 8.8 $ng.g^{-1}$, respectively) and 3) in gills at 30 days (52.0 ± 8.6 and 37.1 ± 7.8 $ng.g^{-1}$, respectively) (Mann-

Whitney test, p<0,05, Table S4 and S5). The concentration of ^{199}Hg(II) at 30 days was lower in the remaining tissues reared at lowered pH (1.3 ± 0.3 and 3.7 ± 1.4 ng.g^{-1} at pH 7.54 and 8.1 respectively, Mann-Whitney test, p<0.05, Table S5). Following the weak influence of pH on bioaccumulation and transformations of Hg species in cuttlefish in this study, the data from both pH conditions were pooled for the rest of the analysis on Hg bioaccumulation and *in vivo* transformation.

3.2 Kinetics of Hg species bioaccumulation in cuttlefish

Using a mass budget approach and thus avoiding interpretation bias on Hg concentrations affected by the important growth of cuttlefish during the experiment (i.e. dilution effect), the accumulation of each enriched isotope of Hg (^{199}Hg, ^{202}Hg) under either organic (MeHg) and inorganic (Hg(II)) form were determined in the brain, digestive gland, gut, gills and the remaining tissues of cuttlefish after 10, 20 and 30 days of exposure (only at 30 days for the remaining tissues) (Figure 2).

Methylmercury (both ^{199}Hg and ^{202}Hg isotopes) accumulated constantly after 10, 20 and 30 days of exposure in all organs but the digestive gland. Based on Me^{202}Hg quantities reached at end of the exposure, organs were ranked from the highest to the lowest contaminated as follow: 55.4 ± 3.4 ng in remaining tissues > 51.4 ± 3.4 ng in mantle > 16.7 ± 1.9 ng in gut ~ 15.7 ± 1.1 ng in digestive gland > 3.3 ± 0.2 ng in gills > 2.0 ± 0.1 ng in brain. In the digestive gland, MeHg values were relatively constant during the 30 days of exposure (with a maximum value: 17.3 ± 3.6 ng at 20 days) and was 6-fold lower than this of Hg(II) at 30 days. Inorganic Hg(II) bioaccumulation (both enriched spikes with ^{199}Hg and ^{202}Hg isotopes) remained very low in all organs (with a maximum value: 20.4 ± 4.4 ng $^{199+202}$Hg(II) in the remaining tissues at 30 days), except in the digestive gland where Hg(II) increased linearly during the 30 days of the experiment reaching 100.4 ± 4.9 ng ^{199}Hg(II) at the end.

The net Hg(II) and MeHg bioaccumulation by the whole organism after 30 days of exposure were deducted from the isotopes mass budget calculation in the whole cuttlefish (addition of ^{199}Hg and ^{202}Hg isotopes for each Hg form) divided by the theoretical quantity of each enriched isotopes ingested by cuttlefish during 30 days (Table S1). The estimation of bioaccumulation efficiency (BE) reached 86% for MeHg and 34% for Hg(II) (see sup data section 1.4).

3.3 In vivo Hg transformations

The percentages of ^{202}Hg(II) and Me^{199}Hg newly formed during the experiment were calculated for each organ and after each time of exposure (Table 1, see sup data for details). Few quantities of ^{199}Hg(II) were methylated *in vivo* in cuttlefish: the majority of Me^{199}Hg was observed in brain and represented 32± 4% and 36± 8% of a low total ^{199}Hg quantity (i.e. 0.12 ng) measured in this organ at 20 days and 30 days of exposure, respectively. At the level of the whole organism, this process appears negligible with 0.42% of total ^{199}Hg(II) methylated in Me^{199}Hg. The formation of ^{202}Hg(II), meaning an *in vivo* demethylation process, was mainly observed after 30 days of exposure in the digestive gland and in the remaining tissues, with 20±2% and 21±3% of total measured respectively, and in a lesser proportion in other organs (maximum value for the 30-day exposure: 5.1±1.5% in gut and 4.5±1.4% in brain). The demethylation process in the whole organism reaches 12.98%.

3.4 Mercury metabolism modelling

Despite the complexity of the model, the inference process converged, and thin posterior distributions were obtained for each kinetic and growth parameter suggesting that data provide sufficient information to accurately estimate the model parameters. The median model predictions, superimposed to observed data, are represented in Figure S2 for each isotope form (all organs together), in Figure S3 for each organ (all Hg forms together) and in Figure S4 for

the growth kinetic of each organ. The most important parameters (those estimated at "high" values compared to the others, i.e. >0.001) are summarized in the general scheme reflecting MeHg and Hg(II) management among tissues during time (Figure 1, solid arrows). The gut and digestive gland appear to be key organs for MeHg diffusion to storage organs (mantle, remaining tissues, brain) and Hg(II) removal (gut) and sequestration (digestive gland). The gills appear to be more involved in the removal of MeHg and Hg(II) than in their storage. The formation of demethylated MeHg (^{202}Hg(II)) was primarily predicted in the digestive gland ($kd_{,2}$), followed by the brain ($kd_{,3}$) and remaining tissues ($kd_{,6}$), whereas methylated Hg(II) (Me^{199}Hg) did not appear to be a significant process in any of the organs.

3.5 Microorganisms in the gut and digestive gland of cuttlefish

The 16S rRNA diversity from gut and digestive gland was assessed in cuttlefish at the beginning of the experiment (T0), at T10 and T30 in juveniles from all conditions, and at T20 for cuttlefish from control and Hg condition. These data were compared to microbial diversity found in juvenile and adult cuttlefish sampled in the field (Figure 3). The results showed that intestinal microbiota of cuttlefish was sparsely diversified, the most abundant prokaryotes being representatives of *Mycoplasma* sp. in all experimental conditions (from 89 to 100%, see figure 3A). The only exception was for the control and Hg+pH conditions at 30 days, where bacteria belonging to *Rickettsiaceae* family dominated the 16S rRNA diversity (71% for (1)-T30 and 61% for (4)-T30). The intestinal microbiota diversity of individuals maintained in experimental conditions was relatively similar to that observed in adult and in juvenile cuttlefish collected in the field (99% and 67% of *Mycoplasma sp.*, respectively, Figure 3A), during the same sampling campaign. The digestive gland microbiota (Figure 3B) showed a higher diversity than the gut of cuttlefish, mainly constituted of bacteria belonging to *Mycoplasmataceae* and *Burkholderiaceae* families (maximum values: 89% in control condition (1)-T20 and 63% in pH

condition (3)-T10, respectively), and in a lesser proportion to *Rickettsiaceae* and *Spiroplasmataceae* families (maximum values: 91% in control condition (1)-T30 and 28% in Hg condition (2)-T30, respectively). Overall, the main result is that neither Hg exposure nor decreased seawater pH influenced the composition of the microbiota in gut and digestive gland.

4 Discussion

4.1 *Weak influence of seawater acidification on Hg metabolism in cuttlefish*

Despite the lack of effect of pH on Hg bioavailability in seawater [51], several studies show that ocean acidification leads to a decrease in the bioaccumulation of Hg(II), mainly through direct pathway exposure (dissolved $HgCl_2$) in copepods [35,52,53] and in polychaetes [54], suggesting that biological / physiological response to ocean acidification could affect Hg bioaccumulation efficiency. These authors show that this lower bioaccumulation is linked to an activation of several defense mechanisms (such as the production of repairing / removing damaged proteins) and an oxidative stress response, caused by the drop in pH [35,54]. In addition, the digestive physiology might be affected by hypercarpnia as shown in fish larvae [55], and thus potentially modified Hg assimilation. To the best of our knowledge, influence of pH on trophic Hg(II) exposure in marine organism was never tested before. Few studies related the impact of ocean acidification after trophic MeHg contamination in organisms. Camacho et al. (2020) [56] shows a decrease of MeHg level in the different tissues of the flat Senegalese sole *Solea senegalensis* (liver, brain, muscle), exposed through the trophic pathway (contaminated feed: 8.51 ± 0.15 mg MeHg. kg^{-1} dw), when pH was low (pH ~ 7.6 equivalent to 1400 µatm) after 28 days of exposure and one additional depurative week. In the meagre *Argyrosomus regius*, Sampaio et al. (2018) [39] found that co-occurring ocean acidification (pH ~ 7.5 equivalent to 1500 µatm) decreased MeHg bioaccumulation (contaminated feed: 8.02 mg MeHg. kg^{-1} dw) and contributed to physiological homeostasis and a dampening effect on

oxidative stress response, after 30 days of diet-contaminated exposure. In contrast to these two studies, we observe an increase in $Me^{202}Hg$ concentrations with low pH after 10 days and only in two organs, an effect that is not observed thereafter.

In our study, the weak influence of a pH decrease on Hg metabolism in juvenile cuttlefish exposed to environmental concentrations indicates a certain physiological plasticity of this cephalopod species with respect to pCO_2 variations.

4.2. Different metabolization of MeHg and Hg(II) in cuttlefish

Based on Hg mass budget, we showed that MeHg is easily bioaccumulated in cuttlefish through dietary route, unlike Hg(II). This difference of bioaccumulation reflects the dissimilar metabolization of Hg(II) and MeHg that has been demonstrated in previous works for fish [57,58].

Several studies related a bioaccumulation efficiency (BE) around 90% for MeHg in the freshwater fish Tilapia [34, 59], which is comparable with our results. Regarding $Me^{202}Hg$, the stable amount found in the digestive gland while cuttlefish were constantly exposed to MeHg was consistent with its progressive diffusion toward other tissues, whose quantities increased over the experiment course. The Hg TK model confirms these results, with mainly a significant flow of $Me^{202}Hg$ from the digestive gland to the mantle, remaining tissues and brain. Not surprisingly, the highest $Me^{202}Hg$ proportion was observed in mantle (or muscular part) and in the remaining tissues after 30 days of exposure. The remaining tissues include the muscular arms and branchial hearts which can display high MeHg concentrations [29,31]. Regarding MeHg removal pathways, the Hg TK model indicates that the gills would be able to significantly remove MeHg, although weakly. This is in agreement with the low MeHg concentrations measured in this tissue.

In our study, the BE for Hg(II) is relatively high compared to other species: indeed, Yang et al. (2021) [59] estimated the BE in Tilapia around 5% and Wang et al. (2013) [34] at 10% in the same fish species, showing some variability, probably due to the Hg composition of food. In cephalopods, few experimental works quantified the Hg(II) bioaccumulation through trophic pathway, as studies generally focused on waterborne Hg(II) contamination [30,18]. Nevertheless, using radiolabeled ^{203}Hg(II) enriched artemia fed to newborn juvenile cuttlefish, Lacoue-Labarthe et al (2009) [30] showed that more than 90% of Hg(II) was assimilated but rapidly eliminated with a biological half-life ($Tb_{1/2}$) of 4 days. Despite this rapid elimination, diet contributed to more than 70% of the total Hg(II) accumulation compared to the dissolved pathway. This shows the importance of considering the type of prey for the assessment of the bioaccumulation efficiency of Hg in a given species [26]. The quasi totality of assimilated Hg(II) was retained by the digestive gland, as confirmed by the TK model, probably bound to metalloproteins having a high affinity for this element [19]. Regarding Hg(II) removal pathway, the Hg TK model indicates that the gut and gills would be involved in Hg(II) elimination.

4.3. In vivo Hg transformations in cuttlefish: the major role of digestive gland in MeHg demethylation

The *in vivo* Hg methylation is negligible comparatively to Hg food uptake, since in the whole organisms Hg methylation extent is close to zero (0.42%), as confirmed by the TK model. However, *in vivo* Hg demethylation is estimated at 13%. There is therefore an internal process allowing the MeHg demethylation in cuttlefish, which occurs first in the digestive gland (19.7±1.5%) and secondly in the remaining tissues (21.2 ± 3.1%) and the brain (4.5 ± 1.4%), in accordance with the TK model (with significant demethylation rates of MeHg by the digestive gland, remaining tissues and brain). The digestive gland of cephalopods has several functions, among them the storage and detoxification of pollutants [19,60], as it has been demonstrated

for fish [57,59]. Once demethylated, the newly formed Hg(II) could be directly eliminated, bound to metalloproteins or relocated to other tissues through blood, as it has been proposed for fish [61,62]. A low ^{202}Hg(II) proportion, compared to the digestive gland but similar to the brain, was measured in intestine (5.1±1.5 %), suggests a neglectable contribution of gut to MeHg demethylation but more a ^{202}Hg(II) relocation, confirmed by the TK model. On the contrary, Wang et al (2017) [35] shows that gut is the main organ involved in MeHg demethylation in the fish *Acanthopagrus schlegeli*.

Considering a more dynamic view of the Hg mass budget, our results confirm that one fraction of assimilated Hg(II) is eliminated (theoretical elimination rate k_e = 0.078 d^{-1}, a value consistent with [26,30] and all the eliminated MeHg is due to MeHg demethylation (theoretical demethylation rate k_d = 0.033 d^{-1}), indicating in the same way that direct elimination of MeHg is negligible (section 1.4.3 in sup data for details). Methylmercury demethylation molecular mechanisms remained to explore. Finally, it is noteworthy that MeHg demethylation rate could be affected by the ontogenic stage as juvenile displayed a high metabolism coupled with high growth rates (see Fig S4).

4.4 Involvement of gut and digestive gland microbiota in Hg metabolism

4.4.1 Absence of microbiota sensitivity to both stressors, ocean acidification and Hg

The analysis of the gut microbiota diversity in cuttlefish revealed a very simple microbiome, with *Mycoplasma* sp. being the most abundant genus of bacteria, as observed by Lutz et al. (2019) [63] and Ramirez et al. (2019) [64]. To our knowledge, it is the first study highlighting the presence of a microbiome associated with the digestive gland of cuttlefish. This microbiome is diverse when compared to the gut microbiome. The observed variability seemed to be individual-specific and unrelated to Hg exposure or rearing under lowered seawater pH or both combined stressors (for example, the diversity of *Burkholderiaceae* in the digestive gland

shows high variability for replicates of the T10_Hg condition = 41.8±32.6 %, n=3). Nevertheless, it is recognized that Hg could create a dysbiosis on intestinal microbiota [65,66], which was not observed in this study. This absence of perturbation in microbiota diversity could be explained by the environmental levels of Hg(II) and MeHg used along the exposure period. The cuttlefish microbiota also did not seem specifically sensitive to decreasing pH / increasing pCO_2, whereas ocean acidification induced changes in microbial communities of oyster larvae [67,40]. This seems to confirm a certain plasticity of cuttlefish facing climate change [68].

4.4.2. Bacterial families known to be involved in Hg transformations

Neither the gut nor the digestive gland was characterized by the presence of bacteria involved in Hg methylation. Only the gut of one *in situ* juvenile contained *Desulfobacterota* members but at low abundance (5.82 %). However, it could be that some biotic methylation occurs *in situ* but not during the controlled conditions of the experiment. Some of the microorganisms present in the digestive gland are known to be involved in Hg demethylation through the *mer* operon. Nevertheless, the demethylation, associated with the organomercurial lyase (MerB) would be associated with a loss of mercury through mercury reduction (MerA) which is not the case here. In addition, Hg concentrations were very low in our study and Yang et al. (2021) [59] suggested a minimum level of Hg (MeHg and Hg(II)) for demethylating bacteria are "activated". The observed demethylation, mainly in the digestive gland, is therefore probably due to other biologically or abiotically induced mechanisms. The oxidative demethylation was unlikely to be one of these mechanisms since known methylotrophs were absent from the community apart from one replicate and at low abundance (3.7%). Thus, we hypothesize that demethylation could be due to biologically induced reactions or to abiotic reactions [69]. In the *in situ* environment, cuttlefish live in contact with the sediment which naturally contains sulfide.

Due to the ingestion of sulfide by cuttlefish, demethylation may be higher than that found in this experiment.

This work indicates that predicted climate change scenarios concerning ocean acidification may not impact significantly Hg bioaccumulation and metabolism in cuttlefish. However, interaction between stressors need to be deeply investigated to fully understand the impact on these organisms. This is the first study to investigate and quantify the Hg methylation and demethylation processes in cephalopods and with an "*in vivo* method". Internal Hg demethylation was highlighted, mainly in the digestive gland. Although a microbiome is present in this organ, the origin of this demethylation does not seem due to microbial activity based on our experimental conditions. *In vivo* methylation through bacterial activity also seems not possible in the gut. Hg biotic transformations need to be confirmed with the search of Hgc and Mer genes in *in situ* cuttlefish in contact with sediment.

Supporting information: Details about methods, additional statistical results, and toxico-kinetic model results.

Acknowledgements: The authors acknowledge technical support provided by the IAEA Monaco-based marine laboratories. The IAEA is grateful for the support provided to its Marine Environment Laboratories by the Government of the Principality of Monaco. The authors thanks François Oberhänsli and Angus Taylor for their help for cuttlefish maintenance. This work is a contribution to the MERCy project funded by *la Fondation pour la Recherche sur la Biodiversité* and the *Ministère de la Transition Ecologique et Solidaire*. The *Région Nouvelle Aquitaine* is acknowledged for its support to the Post-doc and the PhD grants to SG and AM,

respectively through the EXPO project. This work was supported by the project ECONAT Axe 1 - Ressources Marines Littorales: qualité et éco-valorisation, funded by the Contrat de Plan Etat-Région and the CNRS and the European Regional Development Fund through the project QUALIDRIS (Ressources Marines et Littorales: Qualité et Eco-valorisation). The Institut Universitaire de France (IUF) is acknowledged for its support to PB as a Senior Member. This work benefitted from the French GDR "Aquatic Ecotoxicology" framework which aims at fostering stimulating scientific discussions and collaborations for more integrative approaches. Authors warmly thank Antoine and José Lacoue-Labarthe, Jérôme Fort and Fernando Pedraza for their support during field sampling. This contribution was made within the framework of the IAEA CRP on "Applied radioecological tracers to assess coastal and marine ecosystem health" (K41019).

Funding sources: This work was supported by la Fondation pour la Recherche sur la Biodiversité and the Ministère de la Transition Ecologique et Solidaire through the MERCY project, and by the Région Nouvelle-Aquitaine through the EXPO project.

REFERENCES

1. Lamborg, C.H., Hammerschmidt, C.R., Bowman, K.L., Swarr, G.J., Munson, K.M., Ohnemus, D.C., Lam, P.J., Heimbürger, L.E., Rijkenberg, M.J.A, Saito, M. A. (2014) A global ocean inventory of anthropogenic mercury based on water column measurements. Nature, 512(7512): 65-68.

2. Jiskra, M., Heimbürger-Boavida, L.E., Desgranges, M.M., Petrova, M.V., Dufour, A., Ferreira-Araujo, B., Masbou, J., Chmeleff, J., Thyssen, M., Point, D., Sonke, J.E. (2021)

Mercury stable isotopes constrain atmospheric sources to the ocean. Nature, 597(7878): 678-682.

3. Watras, C.J., Back, R.C., Halvorsen, S., Hudson, R.J.M., Morrison, K.A., Wente, S.P. (1998) Bioaccumulation of mercury in pelagic freshwater food webs. Science of the Total Environment, 219: 183−208.

4. Campbell, L., Verburg, P., Dixon, D.G., Hecky, R.E. (2008) Mercury biomagnification in the food web of Lake Tanganyika (Tanzania, East Africa). Science of the Total Environment, 402 (2–3): 184–191.

5. Dolbec, J., Mergler, D., Sousa Passos, C.J., Sousa de Morais, S., Lebel, J. (2000) Methylmercury exposure affects motor performance of a riverine population of the Tapajos river, Brazilian amazon. International Archives of Occupational and Environmental Health, 73: 195−203.

6. Carta, P., Flore, C., Alinovi, R., Ibba, A., Tocco, M.G., Aru, G., Carta, R., Girei, E., Mutti, A., Lucchini, R., Randaccio, F.S. (2003) Subclinical neurobehavioral abnormalities associated with low level of mercury exposure through fish consumption. NeuroToxicology, 24: 617− 623.

7. Clarkson, T.W., Magos, L. (2006) The toxicology of mercury and its chemical compounds. Critical Reviews in Toxicology, 36(8): 609-662.

8. Clarkson, T.W., Vyas, J.B., Ballatori, N. (2007) Mechanisms of mercury disposition in the body. American Journal of Industrial Medicine, 50(10): 757-764.

9. Bridges, C.C., Zalups, R.K. (2010) Transport of inorganic mercury and methylmercury in target tissues and organs. Journal of Toxicology and Environmental Health, Part B, 13(5): 385-410.

10. Cooley, S., Schoeman, D., Bopp, L., Boyd, P., Donner, S., Ghebrehiwet, D.Y., Ito, S.I., Kiessling, W., Martinetto, P., Ojea, E., Racault, M.F., Rost, B., Skern-Mauritzen, M. (2022) Oceans and Coastal Ecosystems and Their Services. In: Climate Change 2022: Impacts,

Adaptation and Vulnerability. Contribution of Working Group II to the Sixth Assessment Report of the Intergovernmental Panel on Climate Change [H.-O. Pörtner, D.C. Roberts, M. Tignor, E.S. Poloczanska, K. Mintenbeck, A. Alegría, M. Craig, S. Langsdorf, S. Löschke, V. Möller, A. Okem, B. Rama (eds.)]. Cambridge University Press, Cambridge, UK and New York, NY, USA, pp. 379–550, doi:10.1017/9781009325844.005.

11. Ivanina, A.V., Sokolova, I.M. (2015) Interactive effects of metal pollution and ocean acidification on physiology of marine organisms. Current Zoology, 61: 653-668

12. Shi, W., Zhao, X., Han, Y., Che, Z., Chai, X., Liu, G. (2016) Ocean acidification increases cadmium accumulation in marine bivalves: a potential threat to seafood safety. Scientific Reports, 6(1): 20197.

13. Pörtner, H.O., Farrell, A.P. (2008) Physiology and climate change. Science, 322(5902): 690-692.

14. Houlbrèque, F., Reynaud, S., Godinot, C., Oberhänsli, F., Rodolfo-Metalpa, R., Ferrier-Pagès, C. (2015) Ocean acidification reduces feeding rates in the scleractinian coral *Stylophora pistillata*. Limnology and Oceanography, 60(1): 89-99.

15. Rosa, R., Pimentel, M., Galan, J.G., Baptista, M., Lopes, V.M., Couto, A., Guerreiro, M., Sampaio, E., Castro, J., Santos, C., Calado, R., Repolho, T. (2016) Deficit in digestive capabilities of bamboo shark early stages under climate change. Marine Biology, 163: 1-5.

16. Melzner, F., Thomsen, J., Koeve, W., Oschlies, A., Gutowska, M.A., Bange, H.W., Hansen, H.P., Körtzinger, A. (2013). Future ocean acidification will be amplified by hypoxia in coastal habitats. Marine Biology, 160: 1875-1888.

17. Lacoue-Labarthe, T., Martin, S., Oberhänsli, F., Teyssié, J.L., Markich, S., Jeffree, R., Bustamante, P. (2009). Effects of increased pCO_2 and temperature on trace element (Ag, Cd and Zn) bioaccumulation in the eggs of the common cuttlefish, *Sepia officinalis*. Biogeosciences, 6(11): 2561-2573.

18. Lacoue-Labarthe, T., Reveillac, E., Oberhänsli, F., Teyssié, J.L., Jeffree, R., Gattuso, J.P. (2011) Effects of ocean acidification on trace element accumulation in the early-life stages of squid *Loligo vulgaris*. Aquatic Toxicology, 105(1-2): 166-176.

19. Penicaud, V., Lacoue-Labarthe, T., Bustamante, P. (2017) Metal bioaccumulation and detoxification processes in cephalopods: a review. Environmental Research, 155: 123-133.

20. Ganguli, P.M., Conaway, C.H., Swarzenski, P.W., Izbicki, J.A., Flegal, A.R. (2012) Mercury speciation and transport via submarine groundwater discharge at a Southern California coastal lagoon system. Environmental Science & Technology, 46(3): 1480-1488.

21. Ganguli, P.M., Swarzenski, P.W., Dulaiova, H., Glenn, C.R., Flegal, A.R. (2014) Mercury dynamics in a coastal aquifer: Maunalua Bay, O'ahu, Hawai'i. Estuarine, Coastal and Shelf Science, 140: 52-65.

22. Pierce, G.J., Stowasser, G., Hastie, L.C., Bustamante, P. (2008) Geographic, seasonal and ontogenetic variation in cadmium and mercury concentrations in squid (Cephalopoda: Teuthoidea) from UK waters. Ecotoxicology and Environmental Safety, 70(3): 422-432.

23.Chouvelon, T., Spitz, J., Cherel, Y., Caurant, F., Sirmel, R., Mèndez-Fernandez, P., Bustamante, P. (2011) Inter-specific and ontogenic differences in $\delta^{13}C$ and $\delta^{15}N$ values and Hg and Cd concentrations in cephalopods. Marine Ecology Progress Series, 433: 107-120.

24.Lischka, A., Lacoue-Labarthe, T., Hoving, H.J.T., Javidpour, J., Pannell, J.L., Merten, V., Churlaud, C., Bustamante, P. (2018) High cadmium and mercury concentrations in the tissues of the orange-back flying squid, *Sthenoteuthis pteropus*, from the tropical Eastern Atlantic. Ecotoxicology and Environmental Safety, 163: 323-330.

25.Lischka, A., Lacoue-Labarthe, T., Bustamante, P., Piatkowski, U., Hoving, H.J.T. (2020) Trace element analysis reveals bioaccumulation in the squid *Gonatus fabricii* from polar regions of the Atlantic Ocean. Environmental Pollution, 256: 113389.

26. Minet, A., Metian, M., Taylor, A., Gentès, S., Azemard, S., Oberhänsli, F., Swarzenski, P., Bustamante, P., Lacoue-Labarthe, T. (2022) Bioaccumulation of inorganic and organic mercury in the cuttlefish *Sepia officinalis*: Influence of ocean acidification and food type. Environmental Research, 215: 114201.

27. Bustamante, P., Lahaye, V., Durnez, C., Churlaud, C., Caurant, F. (2006) Total and organic Hg concentrations in cephalopods from the North Eastern Atlantic waters: influence of geographical origin and feeding ecology. Science of the Total Environment, 368(2-3): 585-596.

28. Bustamante, P., González, A.F., Rocha, F., Miramand, P., Guerra, A. (2008) Metal and metalloid concentrations in the giant squid *Architeuthis dux* from Iberian waters. Marine Environmental Research, 66(2): 278–287.

29. Seixas, S., Bustamante, P., Pierce, G.J. (2005) Interannual patterns of variation in concentrations of trace elements in arms of *Octopus vulgaris*. Chemosphere, 59: 1113–1124.

30. Lacoue-Labarthe, T., Warnau, M., Oberhänsli, F., Teyssié, J.L., Bustamante, P. (2009) Bioaccumulation of inorganic Hg by the juvenile cuttlefish *Sepia officinalis* exposed to ^{203}Hg radiolabelled seawater and food. Aquatic Biology, 6: 91-98.

31. Raimundo, J., Vale, C., Rosa, R. (2014) Trace element concentrations in the top predator jumbo squid (*Dosidicus gigas*) from the Gulf of California. Ecotoxicology and Environmental Safety, 102: 179-186.

32. Schaefer, J.K., Szczuka, A., Morel, F.M. (2014) Effect of divalent metals on Hg (II) uptake and methylation by bacteria. Environmental Science & Technology, 48(5): 3007-3013.

33. Rudd, J.W., Furutani, A.K.I.R.A., Turner, M.A. (1980) Mercury methylation by fish intestinal contents. Applied and Environmental Microbiology, 40(4): 777-782.

34. Wang, R., Feng, X., Wang, W. (2013) In vivo mercury methylation and demethylation in freshwater tilapia quantified by mercury stable isotopes. Environmental Science & Technology, 47: 7949–7957.

35. Wang, X., Wu, F., Wang, W. (2017) In vivo mercury demethylation in a marine fish (*Acanthopagrus schlegeli*). Environmental Science & Technology 51: 6441–6451.

36. Gilmour, C.C., Podar, M., Bullock, A.L., Graham, A.M., Brown, S.D., Somenahally, A.C., Johs, A., Hurt, R.A. Jr., Bailey, K.L., Elias, D.A. (2013) Mercury methylation by novel microorganisms from new environments. Environmental Science & Technology, 47(20): 11810-11820.

37. Eagles-Smith, C.A., Silbergeld, E.K., Basu, N., Bustamante, P., Diaz-Barriga, F., Hopkins, W.A., Kidd, K.A., Nyland, J.F. (2018) Modulators of mercury risk to wildlife and humans in the context of rapid global change. Ambio, 47: 170-197.

38. Sampaio, E., Maulvault, A.L., Lopes, V.M., Paula, J.R., Barbosa, V., Alves, R., Pousão-Ferreira, P., Repolho, T., Marques, A., Rosa, R. (2016) Habitat selection disruption and lateralization impairment of cryptic flatfish in a warm, acid, and contaminated ocean. Marine Biology, 163: 1-10.

39. Sampaio, E., Lopes, A. R., Francisco, S., Paula, J.R., Pimentel, M., Maulvault, A.L., Repolho, T., Grilo, T.F., Pousao-Ferreira, P., Marques, A., Rosa, R. (2018) Ocean acidification dampens physiological stress response to warming and contamination in a commercially important fish (*Argyrosomus regius*). Science of The Total Environment, 618: 388-398.

40. Fonseca, F., Cerqueira, R., Fuentes, J. (2019) Impact of ocean acidification on the intestinal microbiota of the marine sea bream (*Sparus aurata* L.). Frontiers in Physiology, 10: 1446.

41. Joos, F., Frölicher, T.L., Steinacher, M., Plattner, G-K. (2011) Impact of climate change mitigation on ocean acidification projections. In: Ocean acidification, Oxford University Press, Oxford, pp. 272-288.

42. Helcom (2013) Climate change in the Baltic Sea Area — Helcom thematic assessment in 2013, Baltic Sea Environment Proceedings No 137, Helsinki Commission — Baltic Marine

Environment Protection Commission, Helsinki (http://www.helcom.fi/Lists/Publications/BSEP137.pdf) accessed 27 October 2013.

43. Bindoff, N.L., Cheung, W.W.L., Kairo, J.G. (2019) Changing ocean, marine ecosystems, and dependent communities, in: Pörtner, H.-O., Roberts, D.C., Masson-Delmotte, V., Zhai, P., Tignor , M., Poloczanska, E., Mintenbeck, K., Alegría, A., Nicolai, M., Okem, A., Petzold, J., Rama, B., Weyer, N.M.(eds), IPCC special report on the ocean and cryosphere in a changing climate, Cambridge University Press, Cambridge, UK.

44. Lee, J.-Y., Marotzke, J., Bala, G., Cao, L., Corti, S., Dunne, J.P., Engelbrecht, F., Fischer, E., Fyfe, J.C., Jones, C., Maycock, A., Mutemi, J., Ndiaye, O., Panickal, S., Zhou, T. (2021) Future Global Climate: Scenario-Based Projections and Near- Term Information. In Climate Change 2021: The Physical Science Basis. Contribution of Working Group I to the Sixth Assessment Report of the Intergovernmental Panel on Climate Change [Masson-Delmotte, V., P. Zhai, A. Pirani, S.L. Connors, C. Péan, S. Berger, N. Caud, Y. Chen, L. Goldfarb, M.I. Gomis, M. Huang, K. Leitzell, E. Lonnoy, J.B.R. Matthews, T.K. Maycock, T. Waterfield, O. Yelekçi, R. Yu, and B. Zhou (eds.)]. Cambridge University Press, Cambridge, United Kingdom and New York, NY, USA, pp. 553–672, doi:10.1017/9781009157896.006.

45. Monperrus, M., Rodriguez Gonzalez, P., Amouroux, D., Garcia Alonso, J.I., Donard, O.F. (2008) Evaluating the potential and limitations of double-spiking species-specific isotope dilution analysis for the accurate quantification of mercury species in different environmental matrices. Analytical and Bioanalytical Chemistry, 390(2): 655-666.

46. Clémens, S., Monperrus, M., Donard, O.F., Amouroux, D., Guérin, T. (2011) Mercury speciation analysis in seafood by species-specific isotope dilution: method validation and occurrence data. Analytical and Bioanalytical Chemistry, 401(9): 2699-2711.

47. Rodriguez-Gonzalez, P., Bouchet, S., Monperrus, M., Tessier, E., Amouroux, D. (2013) In situ experiments for element species-specific environmental reactivity of tin and mercury

compounds using isotopic tracers and multiple linear regression. Environmental Science and Pollution Research, 20(3): 1269-1280.

48. Escudié, F., Auer, L., Bernard, M., Mariadassou, M., Cauquil, L., Vidal, K., Maman, S., Hernandez-Raquet, G., Combes, S., Pascal, G. (2017) FROGS, Find; Rapidly; OTUs with Galaxy Solution. Bioinformatics, 34, 1287–1294, doi:10.1093/bioinformatics/btx791.

49. Afgan, E., Baker, D., Batut, B., Van Den Beek, M., Bouvier, D., Čech, M., Chilton, J., Clements, D., Coraor, N., Grüning, B.A, Guerler, A., Hillman-Jackson, J., Hiltemann, S., Jalili, V., Rasche, H., Soranzo, N., Goecks, J., Taylor, J., Nekrutenko, A., Blankenberg, D. (2018) The Galaxy platform for accessible, reproducible and collaborative biomedical analyses: 2018 update. Nucleic Acids Research, 46(W1): W537-W544.

50. Gestin, O., Lacoue-Labarthe, T., Coquery, M., Delorme, N., Garnero, L., Dherret, L., Ciccia, T., Geffard, O., Lopes, C. (2021) One and multi-compartments toxico-kinetic modeling to understand metals' organotropism and fate in *Gammarus fossarum*. Environment International, 156: 106625.

51. Stockdale, A., Tipping, E., Lofts, S., Mortimer, R.J. (2016) Effect of ocean acidification on organic and inorganic speciation of trace metals. Environmental Science & Technology, 50(4): 1906-1913.

52. Wang, M., Chen, J., Lee, Y.H., Lee, J.S., Wang, D. (2021) Projected near-future ocean acidification decreases mercury toxicity in marine copepods. Environmental Pollution, 284: 117140.

53. Li, Y., Wang, W.X., Wang, M. (2017) Alleviation of mercury toxicity to a marine copepod under multigenerational exposure by ocean acidification. Scientific Reports, 7(1): 1-9.

54. Freitas, R., de Marchi, L., Moreira, A., Pestana, J.L., Wrona, F.J., Figueira, E., Soares, A. M. (2017) Physiological and biochemical impacts induced by mercury pollution and seawater acidification in *Hediste diversicolor*. Science of the Total Environment, 595: 691-701.

55. Pimentel, M.S., Faleiro, F., Diniz, M., Machado, J., Pousão-Ferreira, P., Peck, M.A., Rosa, R. (2015). Oxidative stress and digestive enzyme activity of flatfish larvae in a changing ocean. PLoS One, 10(7): e0134082.

56. Camacho, C., Maulvault, A.L., Santos, M.T., Barbosa, V., Fogaça, F.H., Pousão-Ferreira, P., Nunes, M.L., Rosa, R., Marques, A. (2020) Mercury in juvenile *Solea senegalensis*: Linking bioaccumulation, seafood safety, and neuro-oxidative responses under climate change-related stressors. Applied Sciences, 10(6): 1993.

57. Gentès, S., Maury-Brachet, R., Feng, C., Pedrero, Z., Tessier, E., Legeay, A., Mesmer-Dudons, N., Baudrimont, M., Maurice, L., Amouroux, D., Gonzalez, P. (2015) Specific effects of dietary methylmercury and inorganic mercury in zebrafish (*Danio rerio*) determined by genetic, histological, and metallothionein responses. Environmental Science & Technology, 49(24): 14560-14569.

58. Feng, C., Pedrero, Z., Gentès, S., Barre, J., Renedo, M., Tessier, E., Berail, S., Maury-Brachet, R., Mesmer-Dudons, N., Baudrimont, M., Legeay, A., Maurice, L., Gonzalez, P., Amouroux, D. (2015) Specific pathways of dietary methylmercury and inorganic mercury determined by mercury speciation and isotopic composition in zebrafish (*Danio rerio*). Environmental Science & Technology, 49(21): 12984-12993.

59. Yang, T.T., Liu, Y., Tan, S., Wang, W.X., Wang, X. (2021) The role of intestinal microbiota of the marine fish (*Acanthopagrus latus*) in mercury biotransformation. Environmental Pollution, 277: 116768.

60. Rodrigo, A.P., Costa, P.M. (2017) The role of the cephalopod digestive gland in the storage and detoxification of marine pollutants. Frontiers in Physiology, 8: 232.

61. Wang, X., Wang, W.X. (2015) Physiologically based pharmacokinetic model for inorganic and methylmercury in a marine fish. Environmental Science & Technology, 49: 10173-10181.

62. Wang, X., Wang, W.X. (2020) Determination of the low Hg accumulation in rabbitfish (*Siganus canaliculatus*) by various elimination pathways: simulation by a physiologically based pharmacokinetic model. Environmental Science & Technology, 54: 7440-7449.

63. Lutz, H.L., Ramírez-Puebla, S.T., Abbo, L., Durand, A., Schlundt, C., Gottel, N.R., Sjaarda, A.K., Hanlon, R.T., Gilbert, J.A., Mark Welch, J.L. (2019) A simple microbiome in the European common cuttlefish, *Sepia officinalis*. Msystems, 4(4): e00177-19.

64. Ramírez, A.S., Vega-Orellana, O.M., Viver, T., Poveda, J.B., Rosales, R.S., Poveda, C.G., Spergser, J., Szostak, M.P, Caballero, M.J., Ressel, L., Bradbury, J.M., Tavío, M.M., Karthikeyan, S., Amann, R., Konstantinidis, K.T., Rossello-Mora, R. (2019) First description of two moderately halophilic and psychrotolerant Mycoplasma species isolated from cephalopods and proposal of *Mycoplasma marinum* sp. nov. and *Mycoplasma todarodis* sp. nov. Systematic and Applied Microbiology, 42(4): 457-467.

65. Nielsen, K.M., Zhang, Y., Curran, T.E., Magnuson, J.T., Venables, B.J., Durrer, K.E., Allen, M.S., Roberts, A.P. (2018) Alterations to the intestinal microbiome and metabolome of *Pimephales promelas* and *Mus musculus* following exposure to dietary methylmercury. Environmental Science & Technology, 52(15): 8774-8784.

66. Duan, H., Yu, L., Tian, F., Zhai, Q., Fan, L., Chen, W. (2020) Gut microbiota: A target for heavy metal toxicity and a probiotic protective strategy. Science of the Total Environment, 742: 140429.

67. Flores-Higuera, F.A., Luis-Villaseñor, I.E., Rochin-Arenas, J.A., Gómez-Gil, B., Mazón-Suástegui, J.M., Voltolina, D., Medina-Hernández, D. (2019) Effect of pH on the bacterial community present in larvae and spat of Crassostrea gigas. Latin American Journal of Aquatic Research, 47(3): 513-523.

68. Seibel, B.A. (2016) Cephalopod susceptibility to asphyxiation via ocean incalescence, deoxygenation, and acidification. Physiology, 31(6): 418-429.

69. Barkay, T., Gu, B. (2021) Demethylation– the other side of the mercury methylation coin: A critical review. ACS Environmental Au, 2(2): 77-97.

Figures

Abstract art

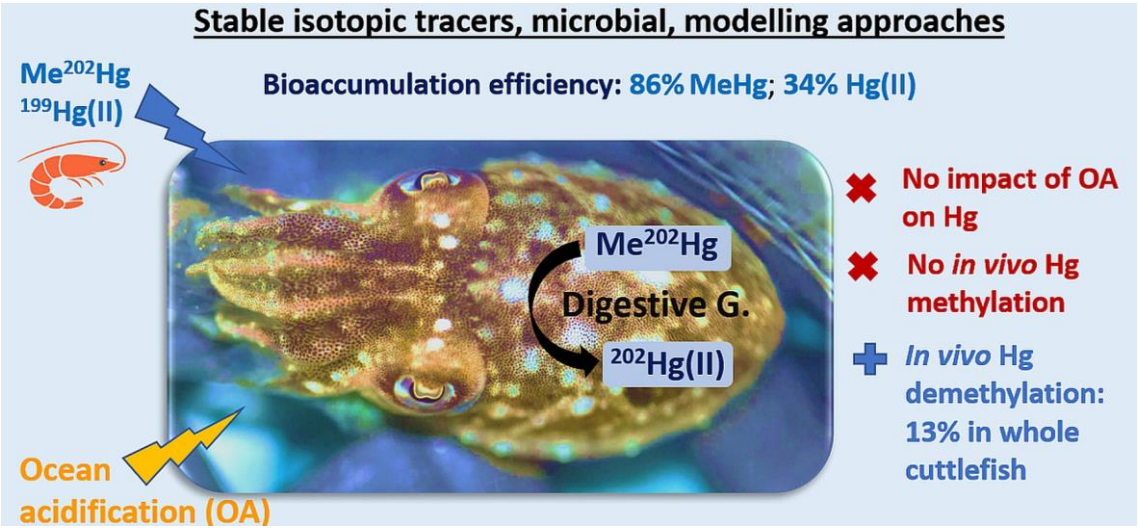

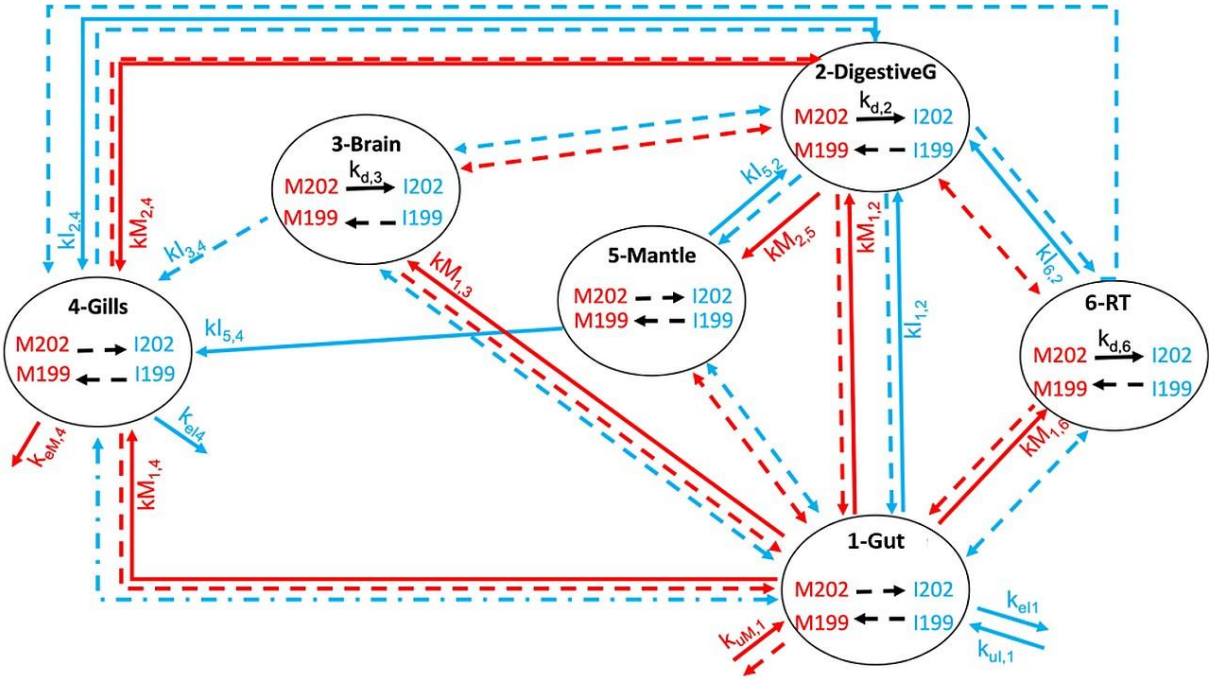

Figure 1. Modelling of *in vivo* mercury isotopes transformations and distribution in different organs of cuttlefish (gills, brain, mantle, digestive gland, intestine and remaining tissues). Dotted arrow: parameters estimated at very low values (<0.001), solid arrow: parameters estimated at high values (>0.001). M: MeHg, I:Hg(II), RT: remaining tissues.

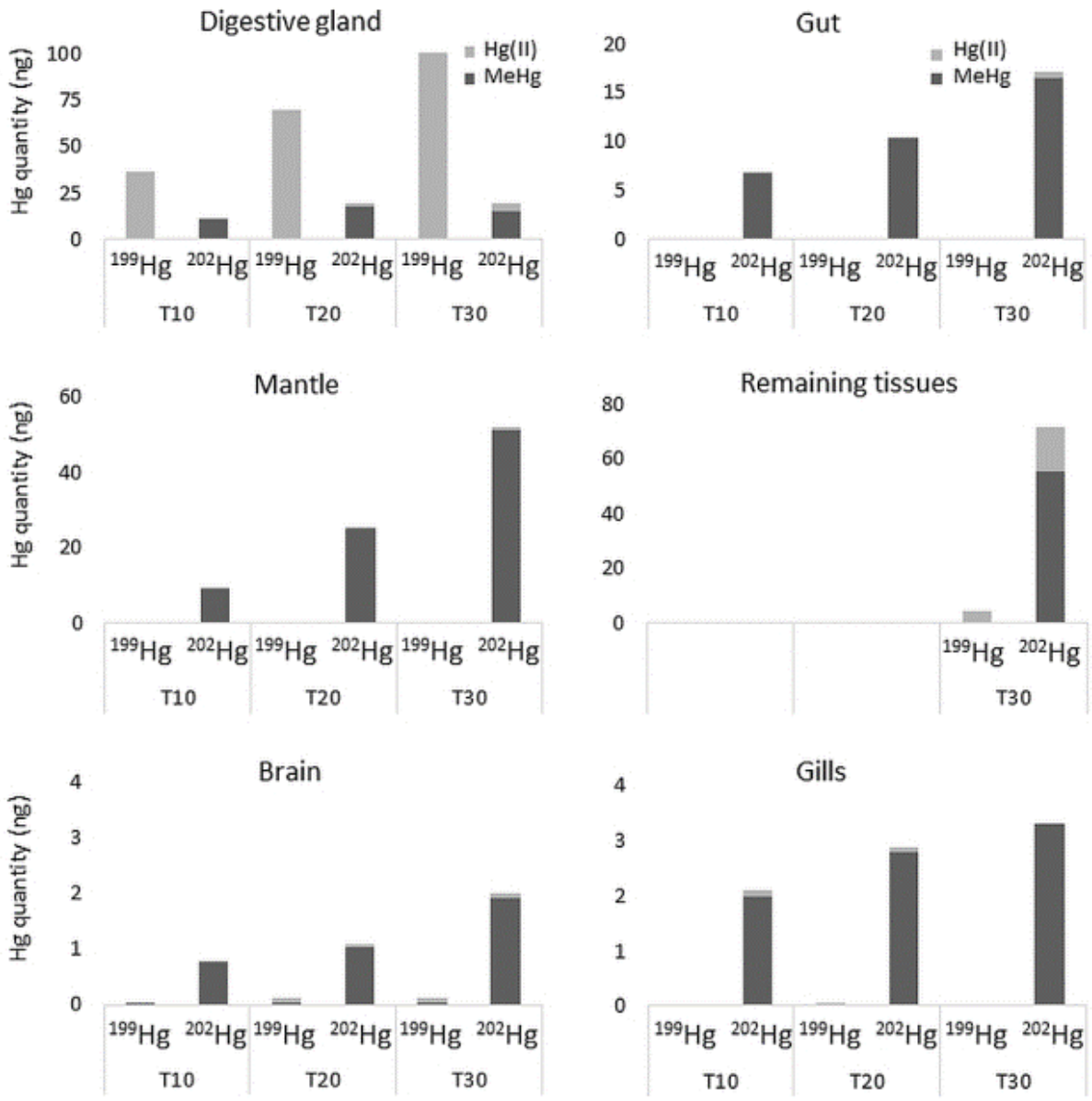

Figure 2. Quantity of Hg isotopes under inorganic (Hg(II)) and methylated forms (MeHg) measured in different organs of cuttlefish at 10, 20 and 30 days (except for the remaining tissues, just at 30 days).

Table 1. Percentage of $Me^{199}Hg$ and $^{202}Hg(II)$ measured in each tissues at 10, 20 and 30 days. Calculations are based on the quantities of the different isotopes of interest. N = number of replicates. Mean ± SE. Values in italics: calculation based on low amounts of isotopes (<1ng), indicating a methylation difficult to quantify (close to zero). "-" means undetectable.

ORGAN	TIME	N	%$Me^{199}Hg$ formed	%$^{202}Hg(II)$ formed
Brain	10	11	-	-
	20	5	*31.7 ± 3.8*	5.1 ± 1.5
	30	10	*36.4 ± 7.9*	4.5 ± 1.4
Digestive gland	10	6	-	9.5 ± 1.5
	20	5	0.2 ± 0.1	11.0 ± 1.6
	30	11	0.4 ± 0.0	19.7 ± 1.5
Gills	10	10	-	5.6 ± 1.6
	20	5	-	3.5 ± 0.8
	30	10	-	
Gut	10	6	-	4.3 ± 1.6
	20	5	-	2.5 ± 0.2
	30	11	-	5.1 ± 1.5
Mantle	10	10	-	4.4 ± 1.5
	20	5	-	1.6 ± 0.5
	30	10	-	1.7 ± 0.2
Remaining tissues	30	10	-	21.2 ± 3.1
Whole cuttlefish	**30**	**10**	**0.42**	**12.98**

A

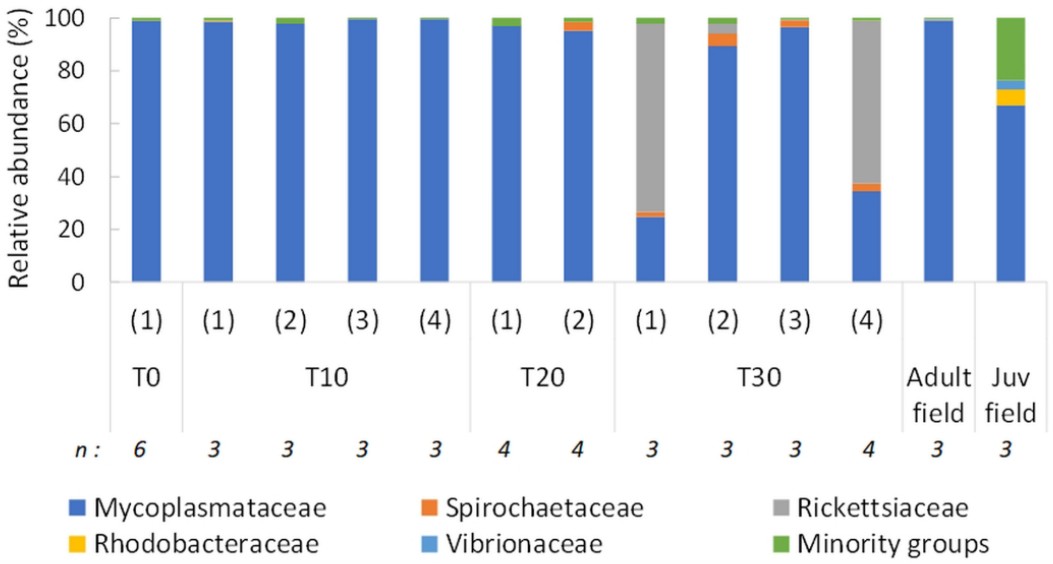

B

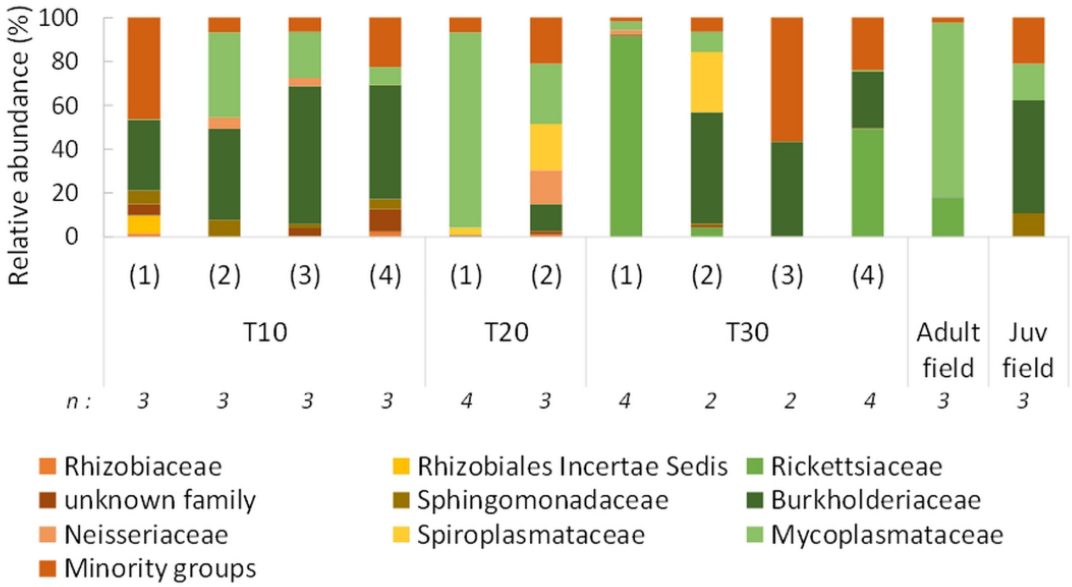

Figure 3. Relative abundance of the most representative microbial family groups (based on 16S rRNA gene) found in gut (A) and digestive gland (B) of cuttlefish in different experimental conditions (1: Control, 2: Hg, 3: pH, 4: Hg+pH) and time (0, 10, 20 and 30 days). "n" indicates number of replicates. Minority groups represent families with relative abundance <4% for gut and <8% for digestive gland (except for T30-pH= 47% of *Cytophagaceae* and T30_Hg+pH= 23% of *Carnobacteriaceae*).

Supporting information

Summary of contents:

1. Methods

1.1. Experimental design

Juvenile cuttlefish were maintained in the Marine Environment Laboratory (International Atomic Energy Agency, Monaco) for 7 days prior to experimentation and fed with the same food as *in situ* (live shrimps *Palaemon varians*) in order to minimize stress due to the change of environment. They were randomly placed in 8 open-water tanks (7 to 9 cuttlefish per tank) containing 20 L of seawater under the following parameters: flux = 60 $L.h^{-1}$; salinity = 38 psu; temperature = 19 ± 0.2°C; pH = 8.1; photoperiod =12h/12h).

The Hg and microbiota analysis were performed on each individual with 5 replicates per experimental condition.

1.2. *Hg injection procedure in shrimps*

Shrimps were sedated in ice water for 1 min minimum and then were intramuscularly injected between the 3rd and 4th abdominal segments (through the articular membrane to minimize breakage of the exoskeleton and clogging of the needle with exoskeleton) with 5 µl of the Hg solution (method developed by Richard A. Neal, http://www.fao.org/3/ac741t/AC741T41.htm). To minimize injury to tissues, the needle (Neuros™ syringe Hamilton 1702 RN, volume: 25µL, gauge: 33) is inserted laterally.

Blue food coloring was added to the Hg solution for checking the injection was correctly made: sedated shrimps were placed on a white wipe (KimTech) for the injection procedure, the blue staining of the paper indicated that the injection was imperfect, and thus the procedure was

repeated with another shrimp. The interaction between Hg and food coloring was tested: the food coloring was chemically inert to the Hg solution. The shrimp was fed directly to the cuttlefish, without passing through an intermediate aqueous medium. If the shrimp was not eaten within a few minutes, it was removed and a new one was presented to the cuttlefish.

To preserve the Hg solution from degradation/transformation during the month of the experiment, aliquots of Hg solution were stored in amber GC vials at -20°C, and one vial was used per day.

1.3. MiSEQ Analysis details

DNA extractions were performed according to the Dneasy PowerSoil Kit (QIAGEN, France) following the manufacturer instructions from 60 to 190 mg of gut and 120 to 440 mg of digestive gland. PCR amplifications were performed with the universal eubacterial 16S rRNA gene primers 8F, 5′- AGAGTTTGATCCTGGCTCAG-3′ and 1492R, 5′-GGTTACCTTGTTACGACTT -3′. The reaction mixture included 0.2 µM of each primer, 2 µl of the sample DNA for gut or 2 µl, 6 µl or 10 µl of the sample DNA for digestive gland (depending on the DNA concentration of the samples), for a final volume of reaction of 25 µl using the AmpliTaq Gold™ 360 Master Mix (Applied Biosystems). The cycle conditions included initial denaturation at 95 °C for 10 min, followed by 25 cycles of denaturation at 95 °C for 40 s, annealing at 55 °C for 40 s, and an elongation at 72 °C for 1 min, and an extension step at 72 °C for 10 min after cycling was complete. Then nested PCR amplifications were performed on the first PCR products: the V4–V5 hypervariable region of the 16S rRNA gene targeting bacteria and archaea was amplified using the primers 515F, 5′-GTGYCAGCMGCCGCGGTA-3′ and 928R, 5′-CCCCGYCAATTCMTTTRAGT-3′. Forwards and reverse primers contained the adapter sequences (CTTTCCCTACACGACGCTCTTCCGATCT) and (GGAGTTCAGACGTGTGCTCTTCCGAT) respectively used in Illumina sequencing technology. 16S rRNA genes fragments were amplified from 2µL of the first PCR with - AmpliTaq Gold™ 360 Master Mix (Applied Biosystems) in the presence of 0.5 µM of primers, in a final volume of 50 µL. The cycle conditions included initial denaturation at 95 °C for 10 min, followed by 30 cycles of denaturation at 95 °C for 30 s, annealing at 65 °C for 30 s, and an elongation at 72 °C for 40 s, and an extension step at 72 °C for 10 min after cycling was complete. Illumina MiSeq 250 bp paired-end sequencing was performed by the Get-PlaGe

sequencing service (INRA, Toulouse, France). After a preprocessing step including quality filter, read trimming, and read assembly, sequences were clustered with Swarm (Mahé et al. 2014) with an aggregation distance of 3 and a denoising clustering step. Operational taxonomic units (OTU) with an abundance lower than 0.005% were removed (Bokulich et al. 2012) in order to delete singletons. The SILVA database 138 (release date 16.12.2019) was used to perform the OTU affiliations (Quast et al. 2012).

References cited:

Bokulich, N.A., Subramanian, S., Faith, J.J., Gevers, D., Gordon, J.I., Knight, R., Mills, D.A., Caporaso, J.G. (2012) Quality-filtering vastly improves diversity estimates from Illumina amplicon sequencing. Nat. Methods, 10: 57–59, doi:10.1038/nmeth.2276.

Mahé, F., Rognes, T., Quince, C., de Vargas, C., Dunthorn, M. (2014) Swarm, robust and fast clustering method for amplicon-based studies. PeerJ, 2: e593, doi:10.7717/peerj.593.

Quast, C., Pruesse, E., Yilmaz, P., Gerken, J., Schweer, T., Yarza, P., Peplies, J., Glöckner, F.O. (2012) The SILVA ribosomal RNA gene database project: improved data processing and web-based tools. Nucleic Acids Research, 41: D590–D596, doi:10.1093/nar/gks1219.

1.4. Calculations of mercury bioaccumulation, transformation and elimination processes

1.4.1. Bioaccumulation efficiency (BE)

$BE_{MeHg=}\Sigma\ Me^{199,202,200}Hg$ in whole organism/ $\Sigma\ Me^{202,200}Hg$ ingested at T30

$BE_{Hg(II)=}\Sigma^{199,202,200}Hg(II)$ in whole organism/ $\Sigma\ ^{199,200}Hg(II)$ ingested at T30,

Calculation based on the average of the isotopes quantities measured at T30 in the different tissues.

1.4.2. Mercury transformations

Hg methylation: $F_{m\%=}\ Me^{199}Hg\ /\ (^{199}Hg(II)+\ Me^{199}Hg)\ *100$

Hg demethylation: $F_{D\%=}\ ^{202}Hg(II)/\ (Me^{202}Hg+^{202}Hg(II))*100$

Calculation based on the sum of the average of the isotopes quantities measured at T30 in the different tissues.

1.4.3. Theoretical elimination rate k_e and theoretical demethylation rate k_d

Cuttlefish ingested 8.7 ng of ^{199}Hg(II) daily for 30 days (261 ng), but at T30 only 105 ng of ^{199}Hg(II) remains in the body, corresponding to a theoretical elimination rate k_e of 0.078 d^{-1}. In turn, the daily ^{202}MeHg intake of cuttlefish is 7.4 ng for 30 days (222 ng) after what at T30, 144 ng of ^{202}MeHg remain in the body. Assuming that all of the ^{202}MeHg eliminated is in fact demethylated, we calculate a demethylation rate k_d of 0.033 d^{-1}. Once demethylated, the newly formed ^{202}Hg(II) (78.7 ng in total) is assumed to be eliminated at the Hg(II) k_e value previously calculated (0.078 d^{-1}). Based on these kinetics parameters, our model shows that 21.2 ng of ^{202}Hg(II) remains unremoved in cuttlefish while 21.4 ng is measured in the mass budget

1.5. <u>Multi-compartments TK model</u>

All tissues growing during the experiment, we consider the dilution by growth in the kinetic model and describe the weight kinetic of each tissue according to the following model:

$$W_i(t) = W_i(0) \times e^{k_{gi} \times t}$$

where $W_i(t)$ is the weight of the tissue i at time t, $W_i(0)$ its weight at the beginning of the experiment (t=0) and k_{gi} its growth rate (i=1…6 : i=1 for intestine, i=2 for digestive gland, i=3 for brain, i=4 for gills, i=5 for mantle and i=6 for rest).

The multi-compartments TK model developed to describe MeHg and Hg(II) concentrations in each tissue during time are expressed as a set of inter-dependent ODE. For the intestines, from which ^{202}MeHg and ^{199}Hg(II) are ingested and can be directly eliminated, we have:

$$\begin{cases} \dfrac{dC_{M202,1}(t)}{dt} = k_{uM1} \times Cf_{M202} + \sum_{j=2}^{6}\left(k_{Mj1} \times C_{M202,j}\right) - \left(\sum_{j=2}^{6} k_{M1j} + k_{eM1} + k_{g1}\right) \times C_{M202,1}(t) - k_{d1} \times C_{M202,1}(t) \\ \dfrac{dC_{I199,1}(t)}{dt} = k_{uI1} \times Cf_{I199} + \sum_{j=2}^{6}\left(k_{Ij1} \times C_{I199,j}\right) - \left(\sum_{j=2}^{6} k_{I1j} + k_{eI1} + k_{g1}\right) \times C_{I199,1}(t) - k_{m1} \times C_{I199,1}(t) \\ \dfrac{dC_{M199,1}(t)}{dt} = \sum_{j=2}^{6}\left(k_{Mj1} \times C_{M199,j}\right) - \left(\sum_{j=2}^{6} k_{M1j} + k_{eM1} + k_{g1}\right) \times C_{M199,1}(t) + k_{m1} \times C_{I199,1}(t) \\ \dfrac{dC_{I202,1}(t)}{dt} = \sum_{j=2}^{6}\left(k_{Ij1} \times C_{I202,j}\right) - \left(\sum_{j=2}^{6} k_{I1j} + k_{eI1} + k_{g1}\right) \times C_{I202,1}(t) + k_{d1} \times C_{M202,1}(t) \end{cases}$$

where $C_{M202,i}(t)$, $C_{I202,i}(t)$, $C_{M199,i}(t)$ and $C_{I199,i}(t)$ correspond to the concentration of ^{202}MeHg, ^{202}Hg(II), ^{199}MeHg and ^{199}Hg(II) into the tissue i (i=1…6 : i=1 for intestine, i=2 for digestive gland, i=3 for brain, i=4 for gills, i=5 for mantle and i=6 for rest) at time t respectively; k_{uM1}, k_{uI1},k_{eM1} and k_{eI1} correspond to the uptake (k_u) and elimination (k_e) rates of ^{202}MeHg, ^{199}Hg(II) for the intestine from the ingested shrimps at the concentrations Cf_{M202} and Cf_{I199} respectively; k_{Mj1} correspond to the transfer rate of MeHg from tissue j to intestine, k_{M1j} to the transfer rate of MeHg from intestine to tissue j; k_{d1} is the demethylation rate of MeHg and k_{m1} the methylation rate of Hg(II) by the intestine; and k_{g1} is the growth rate of intestine.

For the gills (fourth compartment, i=4), uptake is not possible but direct elimination is:

$$\begin{cases} \dfrac{dC_{M202,4}(t)}{dt} = \sum_{j=1,j\neq4}^{6}\left(k_{Mj4}\times C_{M202,j}\right) - \left(\sum_{j=1,j\neq4}^{6} k_{M4j} + k_{eM4} + k_{g4}\right)\times C_{M202,4}(t) - k_{d4}\times C_{M202,4}(t) \\ \dfrac{dC_{I199,4}(t)}{dt} = \sum_{j=1,j\neq4}^{6}\left(k_{Ij4}\times C_{I199,j}\right) - \left(\sum_{j=1,j\neq4}^{6} k_{I4j} + k_{eI4} + k_{g4}\right)\times C_{I199,4}(t) - k_{m4}\times C_{I199,4}(t) \\ \dfrac{dC_{M199,1}(t)}{dt} = \sum_{j=1,j\neq4}^{6}\left(k_{Mj4}\times C_{M199,j}\right) - \left(\sum_{j=1,j\neq4}^{6} k_{M4j} + k_{eM4} + k_{g4}\right)\times C_{M199,4}(t) + k_{m4}\times C_{I199,4}(t) \\ \dfrac{dC_{I202,1}(t)}{dt} = \sum_{j=1,j\neq4}^{6}\left(k_{Ij4}\times C_{I202,j}\right) - \left(\sum_{j=1,j\neq4}^{6} k_{I4j} + k_{eI1} + k_{g4}\right)\times C_{I202,4}(t) + k_{d4}\times C_{M202,4}(t) \end{cases}$$

For the other tissues, uptake and direct elimination are not considered:

$$\begin{cases} \dfrac{dC_{M202,i}(t)}{dt} = \sum_{j\neq i}\left(k_{Mji} \times C_{M202,j}\right) - \left(\sum_{j\neq i} k_{Mij} + k_{gi}\right) \times C_{M202,i}(t) - k_{di} \times C_{M202,i}(t) \\ \dfrac{dC_{I199,i}(t)}{dt} = \sum_{j\neq i}\left(k_{Iji} \times C_{I199,j}\right) - \left(\sum_{j\neq i} k_{Iij} + k_{gi}\right) \times C_{I199,i}(t) - k_{mi} \times C_{I199,i}(t) \\ \dfrac{dC_{M199,i}(t)}{dt} = \sum_{j\neq i}\left(k_{Mji} \times C_{M199,j}\right) - \left(\sum_{j\neq i} k_{Mij} + k_{gi}\right) \times C_{M199,i}(t) + k_{mi} \times C_{I199,i}(t) \\ \dfrac{dC_{I202,1}(t)}{dt} = \sum_{j\neq i}\left(k_{Ij1} \times C_{I202,j}\right) - \left(\sum_{j\neq i} k_{Iij} + k_{gi}\right) \times C_{I202,i}(t) + k_{di} \times C_{M202,i}(t) \end{cases}$$

Where k_{Mji} correspond to the transfer rate of MeHg from tissue *j* to tissue *i*, k_{Mij} to the transfer rate of MeHg from tissue *i* to tissue *j*; k_{di} is the demethylation rate of MeHg and k_{mi} the methylation rate of Hg(II) by the tissue *i*; and k_{gi} is the growth rate of tissue *i*.

For the stochastic part, we assumed a gaussian distribution for the weight and each isotope concentration:

$$\mathrm{W_{obs,i}(t) \sim \mathcal{N}(W_i(t), \sigma_{Wi})}$$

$$\mathrm{C_{obs,i}(t) \sim \mathcal{N}(C_i(t), \sigma_i)}$$

where $W_{obs,i}(t)$ is the weight of tissue *i* measured at time *t*, $\mathcal{N}$ stands for the Normal law, with a mean $W_i(t)$, the weight of the tissue *i* predicted by the growth model at time *t* , and the standard deviation σ_{wi} for the tissue *I*; $C_{obs,i}(t)$ is the observed concentrations into the tissue *i* (*i* =1..6) at time *t*, $C_i(t)$ is the internal concentrations in the tissue *i* predicted by the model (EDO just before) at time *t*, and σ_i is the standard deviation of the Gaussian distribution for the concentration in tissue *i*.

2. Figures and Tables

Table S1. Theoretical quantity of Hg isotopes absorbed per cuttlefish during the experiment.

	Hg isotopes	Theorical average Hg/cuttlefish/day (ng)	theorical average Hg/cuttlefish at 10 days (ng)	theorical average Hg/cuttlefish at 20 days (ng)	theorical average Hg/cuttlefish at 30 days (ng)
Spikes*	^{199}Hg(II)	8.7	87	174	261
	Me^{202}Hg	7.4	74	148	222
	TOTAL	**16.1**	**161**	**322**	**483**
	^{200}Hg(II)	16.7	166.7	333.4	500.1
	Me^{200}Hg	3.5	35.1	70.2	105.3
	TOTAL	**36.3**	**362.8**	**725.6**	**1088.4**
Control**	^{200}Hg(II)	16.7	166.7	333.4	500.1
	Me^{200}Hg	3.5	35.1	70.2	105.3
	TOTAL	**20.2**	**201.8**	**403.6**	**605.4**

* 1 shrimp Hg-contaminated (^{199}Hg and ^{202}Hg) + 2 shrimps uncontaminated (^{200}Hg) per day per cuttlefish; Natural Hg concentration calculation in shrimps is based on the analysis of the ^{200}Hg (shrimp average weight: 0.146 ± 0.034 g dw; 8 ± 1ng Me^{200}Hg.g^{-1} and 38 ± 4 ng ^{200}Hg(II).g^{-1} dw, 15 ± 3% MeHg, n=27).

**3 shrimps uncontaminated per day per cuttlefish.

Table S2. Spikes concentrations, transformations and recoveries just after injection of the Hg solution in shrimps (n=20) and after few minutes or hours of injection of the Hg solution. Concentrations are expressed in $ng.g^{-1}$ dry weight; Average ± SE; R% = spike recovery (%), n = number of individuals, each individuals was analyzed in triplicates.

	[$Me^{202}Hg$]	% D	[$^{199}Hg(II)$]	% M	R% $Me^{202}Hg$	R% $^{199}Hg(II)$	n
after injection	92 ± 6	6 ± 0	153 ± 8	0.0	79 ± 3	112 ± 5	20
after 10 min	35 ± 1	5 ± 2	42 ± 1	0.0	73	75	1
after 3h	33 ± 4	4 ± 1	41 ± 7	0.0	63 ± 10	69 ± 14	4
after 5h	18 ± 1	9 ± 8	19 ± 2	0.0	13	12	1

No methylation and low demethylation processes (explaining decrease in [$Me^{202}Hg$] and loss) have been observed.

A.

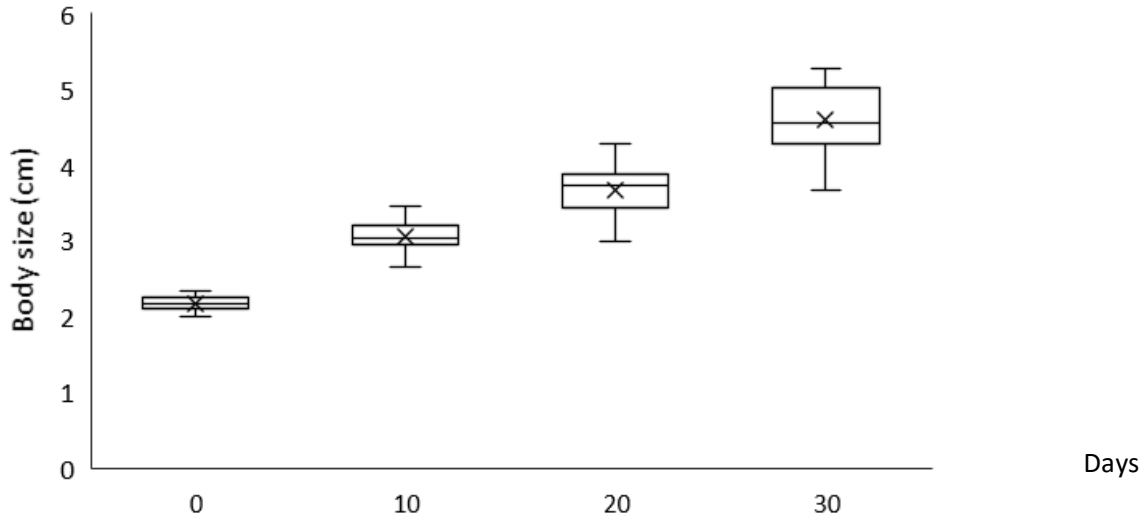

B.

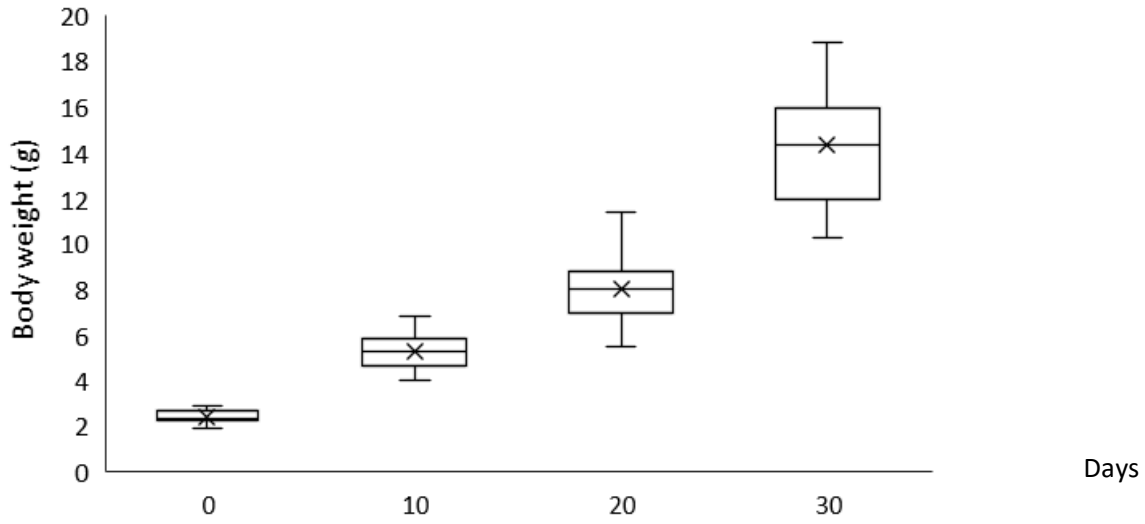

Figure S1. Box plot of size (A) and weight (B) of whole cuttlefishes along the experiment (Day 0 = 9 individuals measured; Day 10 = 24; Days 20 = 12; Days 30 = 28; Total = 73 individuals).

Organisms' health**:** During the experiment, cuttlefish appeared healthy on external inspection (no injury) and no alteration of animals' motility or mortality was observed (n=72). No influence of pH and Hg ("control", "pH", "Hg", "pH+Hg" conditions) were noted on biometric parameters (i.e. size and weight) during the experiment (ANOVA, test LSD fisher, $p>0,05$). The size was 2-fold increased and the average weight was 6-fold higher from the beginning (T0) to the end (T30) of the experiment, all conditions considered (Figure S1).

Table S3. Results of Mann-Whitney test (p-values) on comparison of different variables measured for Hg in Hg contaminated condition and a normal seawater pH (pH = 8.1) and Hg contaminated condition with an acidification of the seawater (pH = 7.54) after 10 days of exposure (T10), in different tissues of cuttlefish. $p < 0.05$ is significant and marked in bold. [ ] indicates concentrations of Hg isotope; %M = percentage of $Me^{199}Hg$ formed; %Demeth = percentage of $^{202}Hg(II)$ formed; $Me^{200}Hg$ and $^{200}Hg(II)$ = "natural" Hg bioaccumulated; %MeHg = percentage of total MeHg compared to total Hg (THg); n = number of replicates in Hg condition ("Hg") and in acidified condition with Hg ("Hg+pH"). NA = not applicable.

T10	Gut	Brain	Mantle	Digestive G.	Gills
[$Me^{199}Hg$]	NA	0.201	0.054	0.268	0.251
[$^{199}Hg(II)$]	0.3758	0.067	0.076	0.513	0.341
%M	0.1213	0.170	0.054	0.513	0.389
[$Me^{202}Hg$]	0.1266	**0.028**	**0.009**	0.513	0.251
[$^{202}Hg(II)$]	0.8273	0.144	0.754	0.513	0.754
%Demeth	0.8273	0.715	0.251	0.513	0.465
[$Me^{200}Hg$]	0.1266	0.273	0.754	0.275	0.251
[$^{200}Hg(II)$]	0.8273	0.715	0.754	0.513	0.175
%MeHg	0.8273	0.715	0.465	0.513	0.602
THg	0.5127	0.855	0.602	0.513	0.117
n Hg / n Hg+pH	3 / 3	5 / 6	5 / 5	3 / 3	5 / 5

Table S4. Results of Mann-Whitney test (p values) on comparison of different variables measured for Hg in Hg contaminated condition (pH = 8.1) and Hg contaminated condition with an acidification of the water (pH = 7.54) after 30 days (T30) of exposure, in different organs of cuttlefish. $p < 0.05$ is significant and marked in bold. [ ] indicates concentrations of Hg isotope; %M = percentage of $Me^{199}Hg$ formed; %Demeth = percentage of $^{202}Hg(II)$ formed; $Me^{200}Hg$ and $^{200}Hg(II)$ = "natural" Hg bioaccumulated; %MeHg = percentage of total MeHg compared to total Hg (THg); n = number of replicates in Hg condition ("Hg") and in acidified condition with Hg ("Hg+pH"). NA = not applicable.

T30	Gut	Brain	Mantle	Digestive gland	Gills	Remaining tissues
$[Me^{199}Hg]$	0.338	0.602	0.597	0.273	0.602	NA
$[^{199}Hg(II)]$	0.314	0.917	0.602	0.273	0.347	**0.016**
%M	0.251	0.751	0.389	0.855	0.834	0.521
$[Me^{202}Hg]$	1.000	0.076	0.175	0.855	**0.028**	0.917
$[^{202}Hg(II)]$	0.715	0.754	0.754	0.855	0.602	0.076
%Demeth	0.584	0.917	0.602	1.000	0.175	0.076
$[Me^{200}Hg]$	0.465	0.465	0.347	0.715	0.347	0.117
$[^{200}Hg(II)]$	0.855	0.117	0.465	0.100	0.754	0.117
%MeHg	0.855	**0.047**	0.917	1.000	0.754	0.117
THg	0.584	0.347	0.465	0.100	0.602	0.465
n Hg / n Hg+pH	6 / 5	5 / 5	5 / 5	6 / 5	5 / 5	5 / 5

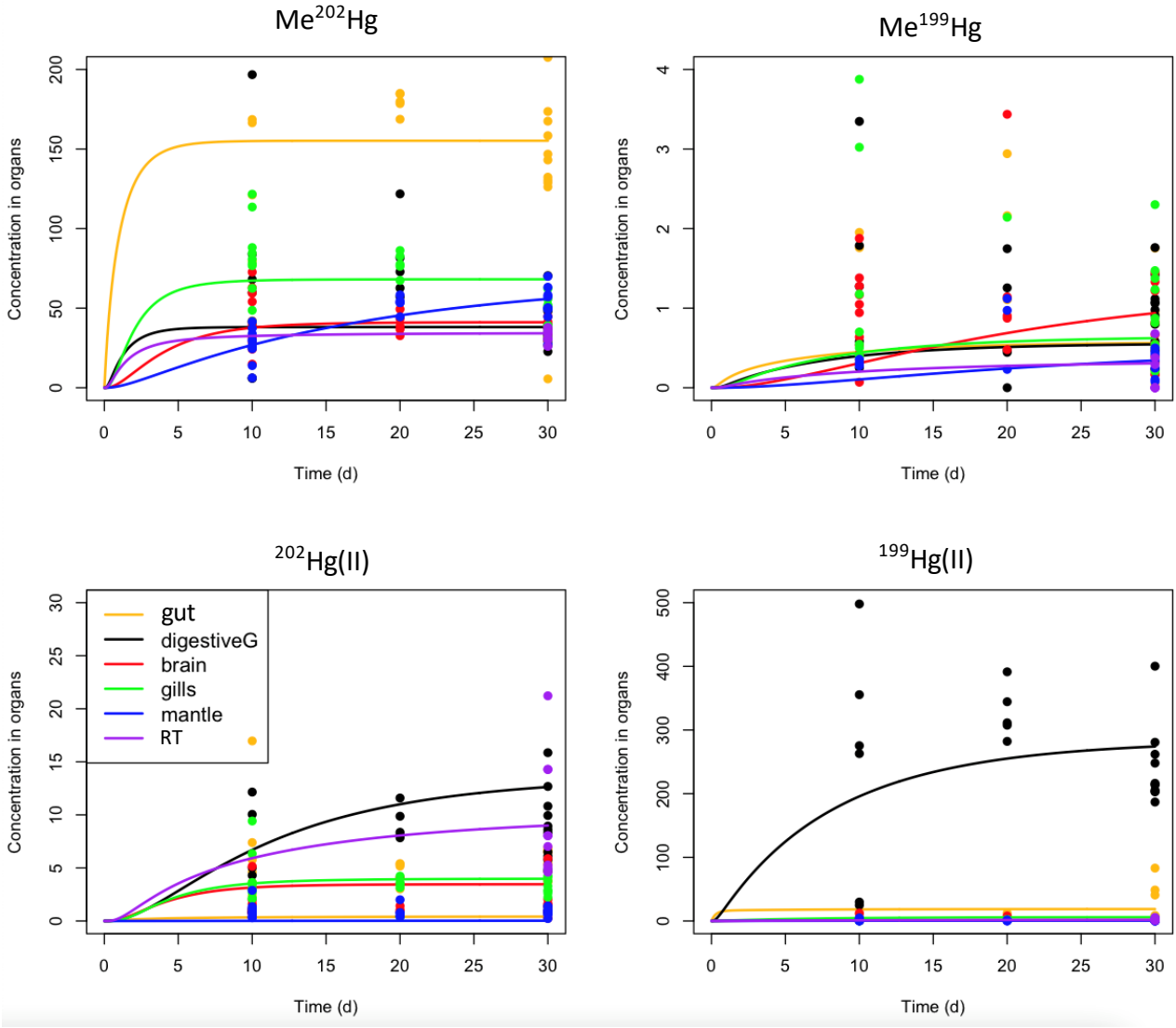

Figure S2. Adjustments of Hg species concentrations (ng.g^{-1} dry weight) measured in different organs of cuttlefish at different time (0, 10, 20 and 30 days), both pH conditions pooled, and based on the TK model. RT: remaining tissues.

A.

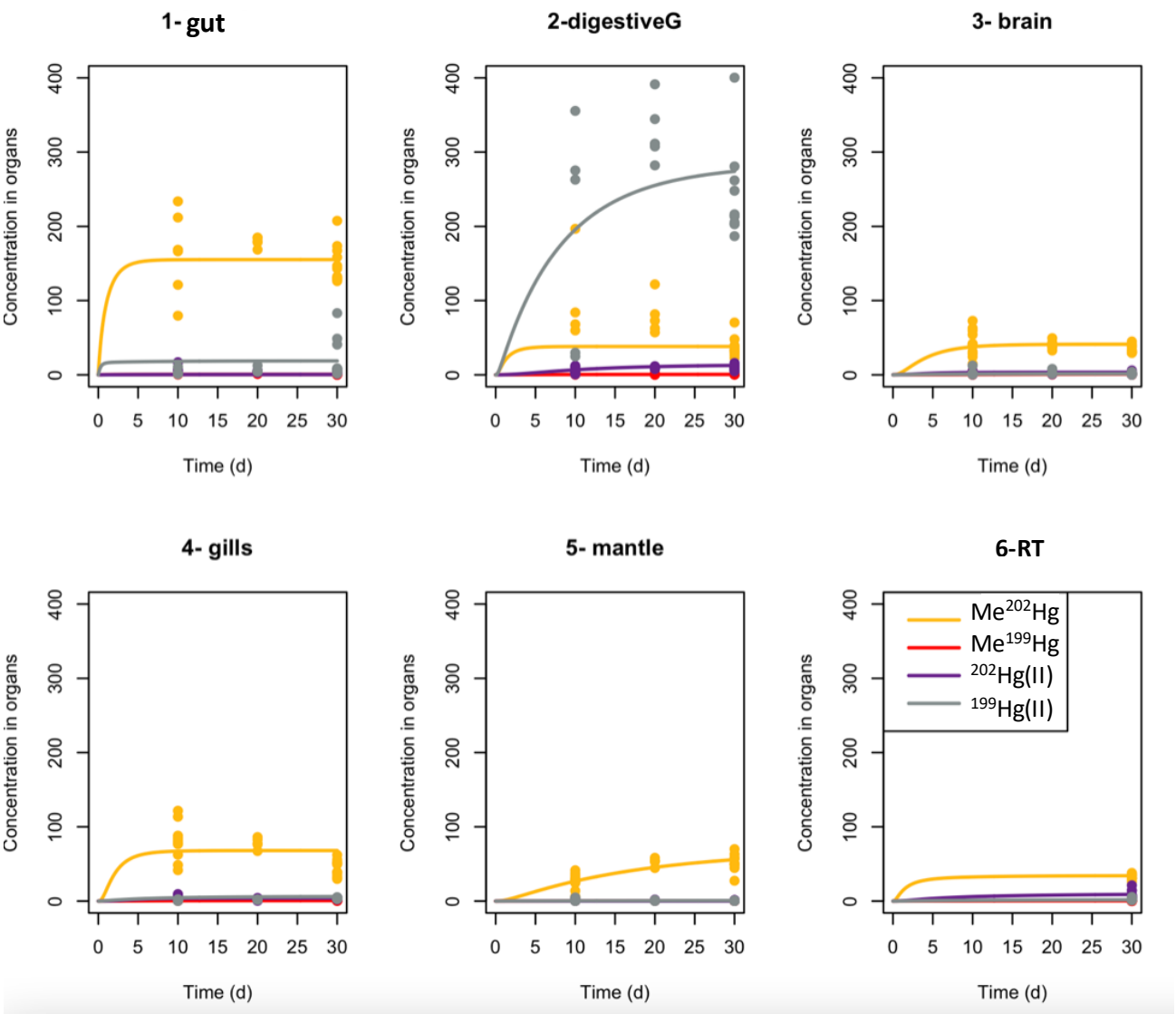
1- gut
2-digestiveG
3- brain
4- gills
5- mantle
6-RT
Concentration in organs
Time (d)
0
100
200
300
400
0 5 10 15 20 25 30
Me202Hg
Me199Hg
202Hg(II)
199Hg(II)

B.

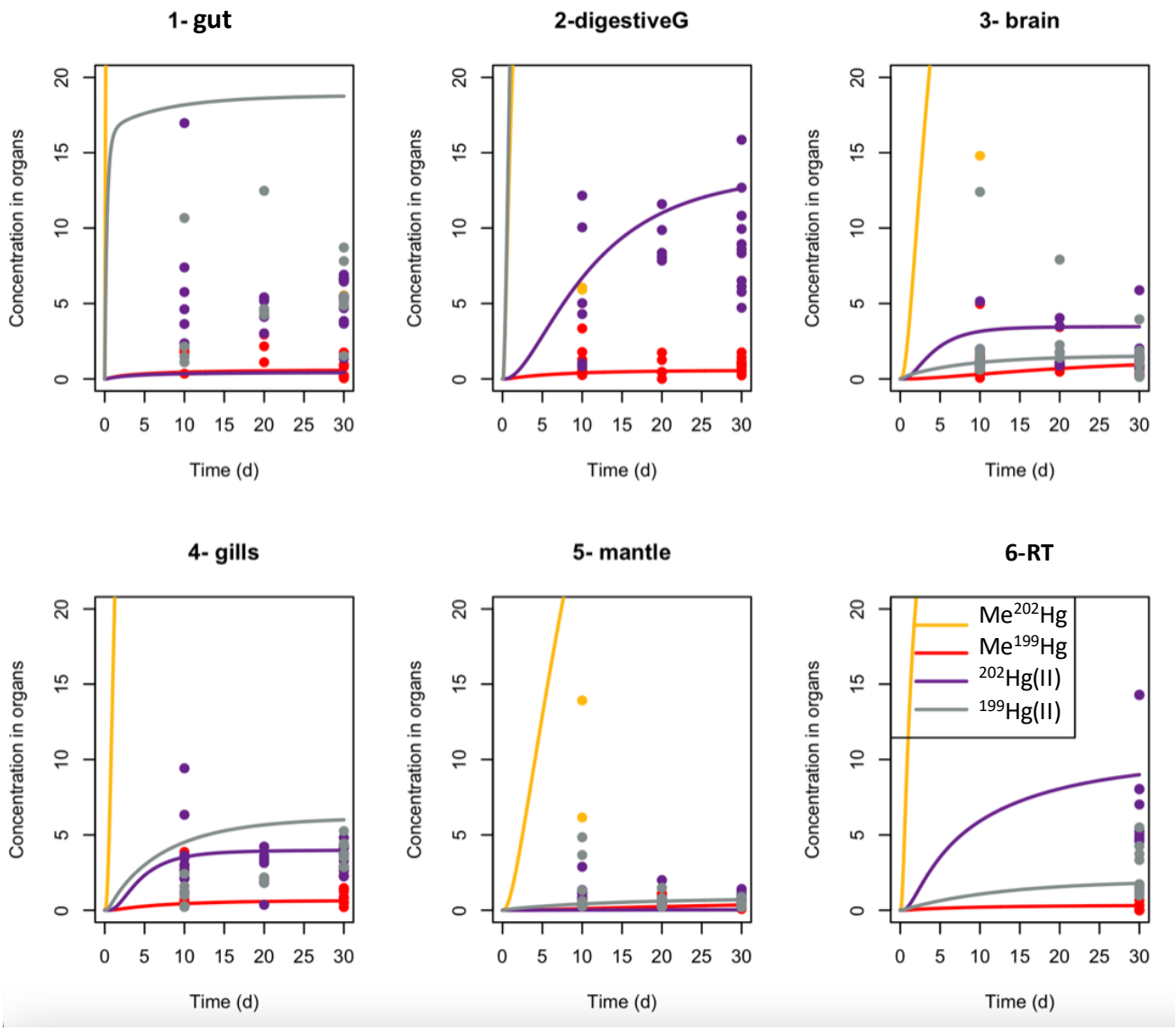

Figure S3. A) Adjustments of Hg species concentrations (ng.g^{-1} dry weight) measured in different organs of cuttlefish at different time (0, 10, 20 and 30 days), both pH conditions pooled and based on the TK model, presented here by organ. B) Scale enlargement for isotopes with the lower concentrations measured. RT: remaining tissues.

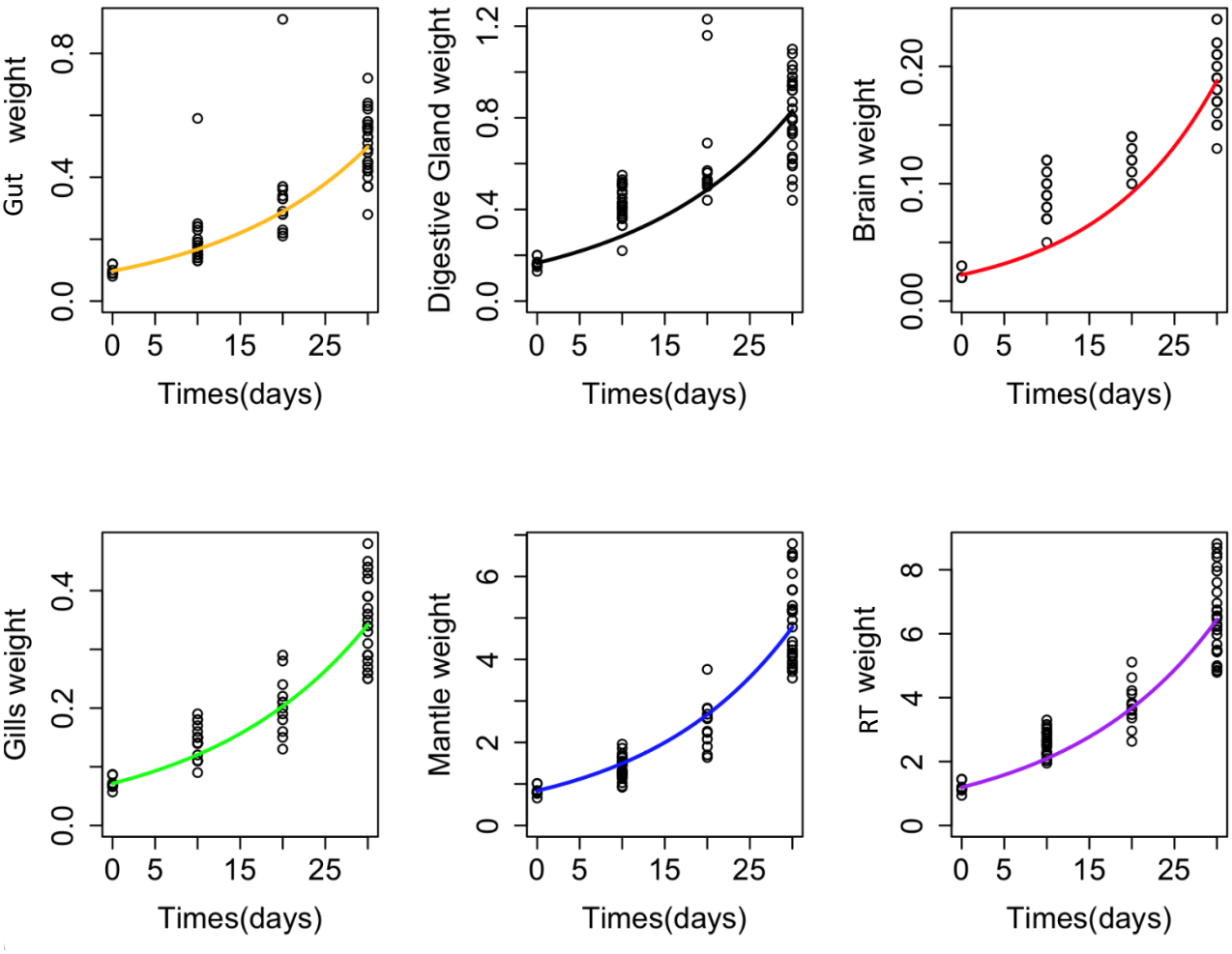

Figure S4. Adjustments of weight (g) for different organs of cuttlefish at different time (0, 10, 20 and 30 days), both pH conditions pooled and based on the TK model. RT: remaining tissues.